ISBN ISBN 978-82-471-1659-3 (printed ver.)
ISBN ISBN 978-82-471-1661-6 (electronic ver.)
ISSN 1503-8181

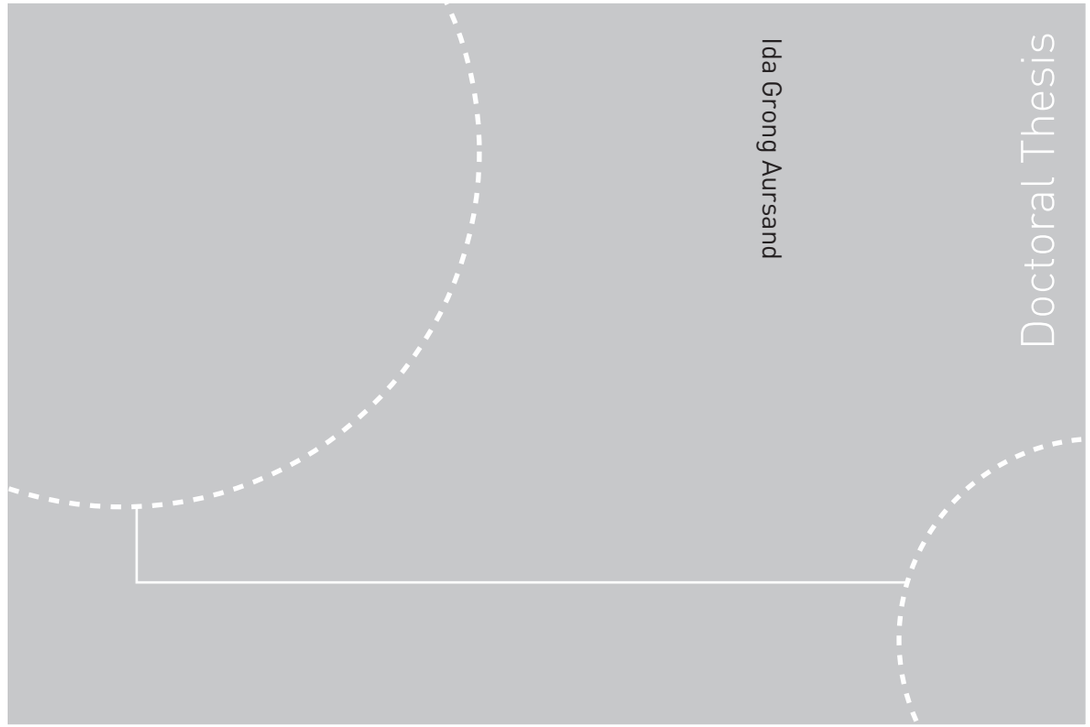

Doctoral theses at NTNU, 2009:136

Ida Grong Aursand

Low-field NMR and MRI studies of fish muscle

Effects of raw material quality and processing

Doctoral theses at NTNU, 2009:136

NTNU
Norwegian University of
Science and Technology
Thesis for the degree of
philosophiae doctor
Faculty of Natural Sciences and Technology
Department of Biotechnology

NTNU
Norwegian University of
Science and Technology

NTNU
Norwegian University of
Science and Technology

Ida Grong Aursand

Low-field NMR and MRI studies of fish muscle

Effects of raw material quality and processing

Thesis for the degree of philosophiae doctor

Trondheim, June 2009

Norwegian University of
Science and Technology
Faculty of Natural Sciences and Technology
Department of Biotechnology

NTNU
Norwegian University of
Science and Technology

NTNU
Norwegian University of Science and Technology

Thesis for the degree of philosophiae doctor

Faculty of Natural Sciences and Technology
Department of Biotechnology

ISBN 978-82-471-1659-3 (printed ver.)
ISBN 978-82-471-1661-6 (electronic ver.)
ISSN 1503-8181

Doctoral Theses at NTNU, 2009:136

Printed by Tapir Uttrykk

Acknowledgements

This thesis is submitted in partial fulfilment of the PhD at the Norwegian University of Science and Technology (NTNU), Department of Biotechnology, and is based on research conducted in the period August 2003 to May 2009. The experimental work of this thesis has been carried out at the SINTEF Fisheries and Aquaculture laboratories, at the MR Centre in Trondheim, and partly at The Norwegian Food Research Institute.

The work was financed by the Matforsk-SINTEF Strategic Institute Programme "Production improvements of salted/cured meat and fish: Development of rapid and non-destructive salt analyses related to production, yield and quality (Project no. 153381/140)" supported by the Research Council of Norway.

First of all I would like to thank my advisor-team. Ulf Erikson, Senior Scientist at SINTEF Fisheries and Aquaculture (SFH), is deeply thanked for his inspiration, his excellent guidance in scientific writing and for sharing his vast of knowledge in the field of aquaculture and fish quality with me. Emil Veliyulin, Scientist at SFH, is thanked for introducing me to the world of NMR, for his participation in the lab work and last but not least for his bottomless helpfulness. Turid Rustad, Prof. at NTNU, is warmly thanked for always having the time to help me and for excellent guidance in all parts of my PhD work.

I would also like to thank my co-authors for the excellent collaboration and valuable discussions. A special 'thank you' goes to Dr. Lorena Gallart-Jornet for the close collaboration in the writing of one of the papers in this thesis. Dr. David Axelson is thanked for his valuable participation in discussions regarding data processing. My gratitude also goes to Marit Aursand, Research director at SINTEF Fisheries and Aquaculture, for her inspiration, motivation and support, and last but not least for her sense of humour.

I am thankful to my colleagues for providing a great environment, both socially and professionally. Especially, I would like to thank Dr. Ekrem and Dr. Inger Beate for being the best office-neighbours through these years and for sharing frustrations and triumphs on the way to becoming doctors.

This PhD was a part of a project originated by SFH, where I have been an employee for six years. It has been challenging to maintain focus on my PhD and industrial projects at the same time, but I am still grateful for what I have learned from this experience, and today I am not in doubt that it was

worth it. In that occasion, I thank all my friends for their patience. Hopefully, you will se more of me in the future.

I thank my parents for their love, for always believing in me, supporting me and making me believe in my self. I'm also deeply grateful to my brother Iver and my sister Eli for caring and encouraging me during the work. Finally, I thank Tord for being there and always supporting me.

Abstract

The present thesis aims at using non-invasive and non-destructive NMR techniques to contribute to a further understanding of fish tissue composition and its characteristics. Moreover, it aims at investigating the water dynamics and the distribution of fat and salt in fish as affected by species, raw material quality and processing from both the chemical and the physical angle at the same time.

The applicability of low-field NMR as a tool for the fish processing industry was investigated. The bench top low-field NMR instrument was found suitable for fat and water determination in small Atlantic salmon (*Salmo salar*) samples, whereas the portable low-field NMR surface scanner (ProFiler) was appropriate for rapid fat determination in minced muscle. Thus, low-field NMR was proven to be good measuring technique, and with the introduction of the NMR surface scanner concept, online quality control may become feasible in the future.

Transversal (T_2) NMR relaxometry has been demonstrated to contain valuable information about water dynamics in Atlantic salmon and Atlantic cod (*Gadus morhua*) tissue. The thesis contributes to a further understanding of the relationship between water distribution and microstructure of fish flesh. It has been established that the method is sensitive to fish species, ante-mortem handling, rigor status, freezing/thawing, heating, and brine salting. The tissue T_2 relaxation characteristics have been linked to microstructure, salt distribution and salt uptake. It is shown that T_2 relaxation components correlate well with water holding capacity during salting. It has been suggested that entrapped and free water, and fat when present, give rise to the main relaxation components in fish muscle tissue. The understanding of the tissue water distribution and dynamics has been improved. However, the clarification of the relaxation characteristics in fish flesh is still an active area of research.

In fatty fish, both fat and water contributes to the T_2 NMR relaxation signal. A two dimensional map of the diffusion versus T_2 relaxation proved to be a good technique to increase the understanding of water and fat distribution in salmon muscle tissue, by clear separation of the NMR signals from water and fat components into different populations.

MR imaging was probed for investigation of fat and salt distribution. ^{1}H MRI was successfully applied to produce separate quantitative water and fat images. Combined ^{1}H and ^{23}Na imaging of brine salted Atlantic salmon revealed that the uptake and distribution of salt in the tissue was highly dependent on the spatial fat distribution.

An evident relation was observed between T_2 relaxation characteristics of salmon flesh and the sodium distribution in salted fillets. T_2 relaxaometry and MR imaging gave further insight into the microstructure and water distribution of fish tissue of different quality and its effect on salt distribution. The combination of these NMR techniques is considered to be a useful tool to increase the understanding of the tissue water distribution and dynamics and for optimization of salting processes.

Table of contents

List of papers

Paper I Aursand, I.G., Veliyulin, E. and Erikson, U. (2006) Low field NMR studies of Atlantic salmon (*Salmo salar*) In: *Modern Magnetic Resonance* (G. A. Webb, Ed.) Springer, The Netherlands, 895-903.

Paper II Veliyulin, E., Aursand, I.G. and Erikson, U. (2005) Study of fat and water content in Atlantic salmon (*Salmo salar*) by low-field NMR and MRI. In: *Magnetic Resonance in Food Science – The multivariate Challenge* (S.B. Engelsen, P.S. Belton and H.J. Jakobsen Eds.), pp 148-155, Special Publication No. 299, The Royal Society of Chemistry, Cambridge.

Paper III Aursand, I.G., Erikson, U. and Veliyulin, E. (2009) Water properties and salt uptake in Atlantic salmon fillets as affected by antemortem stress, rigor mortis, and brine salting. A low-field ^{1}H NMR and ^{1}H/^{23}Na MRI study. Submitted to *Food Chemistry.*

Paper IV Aursand, I.G., Veliyulin, E., Böcker, U., Ofstad, R., Rustad, T. and Erikson, U. (2009) Water and salt distribution in Atlantic salmon (*Salmo salar*) studied by low-field ^{1}H NMR, ^{1}H and ^{23}Na MRI and light microscopy: Effects of raw material quality and brine salting. *Journal of Agricultural and Food Chemistry,* 57*,* 46-54.

Paper V Aursand, I.G., Gallart-Jornet, L., Erikson, U., Axelson D.E. and Rustad, T. (2008) Water distribution in brine salted cod (*Gadus morhua*) and salmon (*Salmo salar*): A low-Field ^{1}H NMR study. *Journal of Agricultural and Food Chemistry,* 56, 6252-6260.

PART 1

1 Introduction

Strong focus on freshness and high product quality is an essential strategy of fisheries and aquaculture. Nowadays, consumers are becoming increasingly aware of all the dietary benefits of marine foods for human health. Maintaining the quality through the whole value chain is one of the most important challenges for the fish industries. Therefore, it is of importance to develop basic knowledge about the effects of treatment along the value chain such as preslaughter conditions, processing and storage on product quality.

Furthermore, there is a clear trend in the international market towards labelling products with information about their composition and quality. This brings about the need to develop standardized analytical techniques to either confirm the information given by the label or to uncover fraud. The composition such as the fat content, and the life-history of the products (the storage and processing conditions to which it was subjected), are amongst the main issues for which no accepted analytical methods have been discovered yet. Modern rapid non-destructive measuring techniques such as nuclear magnetic resonance (NMR) can be important elements on the way to overcome technical challenges towards reliable and verification of the product composition and quality and, last but not least, to create an economically healthy industry. NMR proton relaxometry can provide information about the mobility and compartmentalisation of water and fat in tissues, whereas proton and sodium MR imaging can provide information about spatial distribution of water/fat and salt, respectively. These features, in addition to their non-destructiveness, make them excellent tools in the work of establishing basic knowledge about effects of raw material properties, storage and processing on fish product quality.

In this thesis, low-field proton NMR coupled with proton and sodium MR imaging have been applied to study raw material quality and processing of Atlantic salmon (*Salmo salar*) and Atlantic cod (*Gadus morhua*). In the first section of the thesis (Paper I and II), the composition of salmon muscle tissue is studied, and a non-invasive determination of fat and water of Atlantic salmon (*Salmo salar*) is approached. The second section (Paper III, IV and V) is dedicated to specific cases typical for the Norwegian fish processing industry such as preslaughter conditions, rigor status, freezing-thawing and processing (heating and salting), and their effect on water and salt distributions in the product. The obtained results are enclosed as 5 submitted or published papers in Part 2 of the thesis.

2 Objectives

The main objective of the present thesis was to use non-invasive and non-destructive NMR techniques to contribute to a further understanding of water dynamics and fat and salt distribution, as affected by raw material quality and processing. The specific goals were:

- To investigate the applicability of low-field NMR techniques for determination of total water and fat content for the fish processing industry.
- To apply low-field NMR T_2 relaxation as a tool to increase the understanding of the tissue water distribution in Atlantic salmon (*Salmo salar*) and Atlantic cod (*Gadus morhua*) as affected by raw material quality and processing.
- To apply MR imaging to non-invasively study distribution of fat, water and salt in Atlantic salmon (*Salmo salar*) muscle tissue as affected by raw material quality and processing.
- To broaden the understanding of water and salt dynamics in fish tissue as affected by ante-mortem handling, post-mortem status and processing by combining different NMR techniques.

3 Background

Different fish muscle tissues display both structural and compositional complexity, and the spatial heterogeneity can range from the molecular to the macroscopic. There is an obvious relationship between structural complexity and dynamic changes associated with processing and storage. This chapter is intended to give a brief overview of the fish flesh composition and the effects of freezing/thawing and processing such as heating and salting.

3.1 Fish muscle structure

Fish muscles are divided into myotomes separated from each other by thin sheets or membranes made up of connective tissues (myocommata). Within each myotome, the muscle fibres run approximately parallel to each other, but at varying angles to the myocommata sheets to give the necessary moment for swimming during contraction. The muscle cells are oriented roughly parallel to the longitudinal axis of the fish (Dunajski, 1979), **Figure 1**.

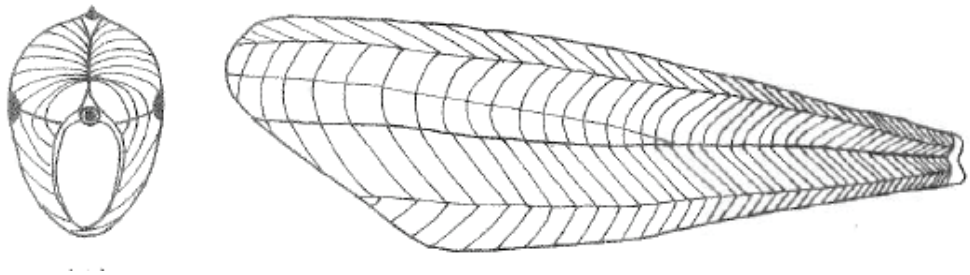

(A) (B)

Figure 1: The metameric structure of a fish muscle. The pattern of the lines on the cross (A) and longitudinal (B) sections represents the arrangement of the sheets of connective tissue in the muscles (Dunajski, 1979).

Fish muscle tissue consists of bundles of cylindrical multinucleated muscle cells. Each muscle cell, also called muscle fibre, is comprised of bundles of myofibrils arranged longitudinally within the muscle cell. In the periphery of the fish cell, the fibrils are elongated with, in cross-section a ribbon-like shape, whereas fibrils in the interior of the cell are roughly polygonal (Howgate, 1979; Bello *et. al*, 1981; 1982), **Figure 2**.

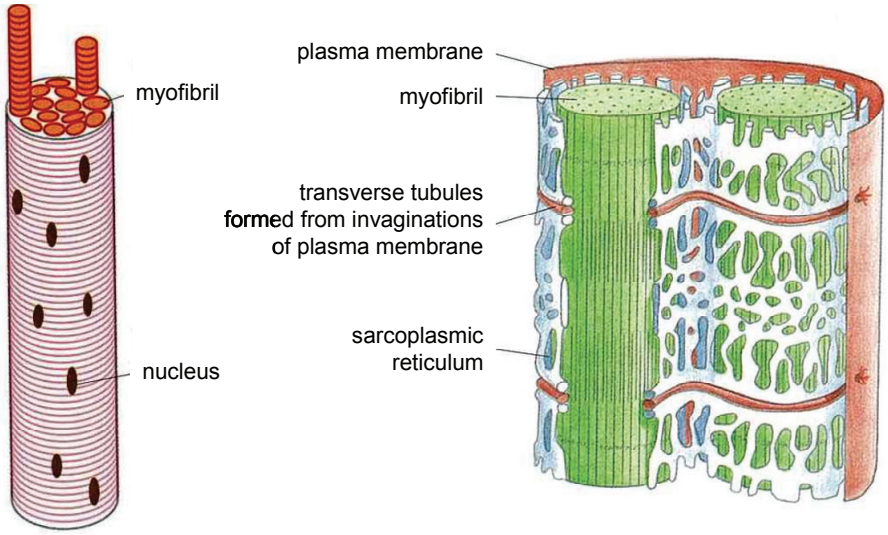

Figure 2: Muscle tissue structure (Alberts et al., 1998).

A fine network of collagen surrounds each muscle fiber and proceeds into the myocommata (Bremner and Hallett, 1985; Bremner, 1992). The collagen content of fish muscle varies considerably between species, and is found in increasing proportion in the tail region. Concentrations of 0.3-3% are common in the main edible proportion, depending on season and nutritional status (Bremner, 1992).

3.2 The principal components of fish flesh

3.2.1 Proteins

The muscle proteins can be divided into three groups, based on solubility properties (Haard, 1992; Foegeding et al., 1996). These are water-soluble or sarcoplasmic proteins (mainly enzymes), salt soluble or myofibrillar proteins (the contractile network) and the insoluble proteins (primarily collagen). Fish flesh contains a relatively high concentration of myofibrillar proteins (70 – 90 %) compared to muscle from land animals (39 – 68 %) (Haard, 1992). This implies that the myofibrillar proteins are important for the water-holding properties of fish muscle. Furthermore, myofibrils occupy around 70% of the volume of lean muscle. Therefore, most of the tissue water is located in the myofibrils (Hamm, 1986). Thus, lateral expansion or shrinking of the filament lattice is expected to greatly influence tissue water distribution and holding capacity, and thus the water mobility. Processing steps such as freezing, salting and cooking are all known to affect the myofibrillar lattice.

3.2.2 Water

Water is the principal component of the fish flesh and the water content is typically in the range of 70 - 80 %. Fresh Atlantic cod (*Gadus morhua*) and Atlantic salmon (*Salmo salar*) contain up to approx. 80 % and 70 % water, respectively. As a key component, water heavily determines the physical characteristics, technological properties, microbial stability, shelf-life and sensory properties. The water-holding is also of great importance, because gains or losses of water affect the weight and therefore the commercial value of fish products.

The majority of the water in muscle tissue is located within the structure of the muscle and the muscle cells. Water is found within and between the myofibrils and between the myofibrils and the cell membrane (sarcolemma), between muscle cells and between muscle bundles (groups of muscle cells) (Offer and Cousins, 1992). The distribution of water in the muscle may be described as divided into three compartments. The 'first' compartment is often named bound water, which contains less than 10% of the water in the muscle. This water is very closely bound to proteins, has reduced mobility and can not easily move to other compartments. The amount of bound water changes very little, if at all, in post-rigor muscle (Offer and Knight, 1988a;b) and it is very resistant to freezing and heating (Fennema, 1990). The 'second' compartment, often called "entrapped" water, is the most affected by the rigor process and the conversion of muscle to meat. This water can eventually escape as drip loss (Offer and Knight, 1988a;b). The 'third' compartment, called "free water", is mainly held by weak surface forces, and is not readily seen in pre-rigor meat, but can gradually develop during and after the rigor process (Fennema, 1990). Together, the "entrapped" and the "free" water, describe approximately 90% of the water in muscle (Offer and Knight, 1988a;b; Fennema, 1985; Cole et al., 1993; Huff-Lonergan and Lonergan, 2005).

The distribution of the water in the muscle tissue 3D network is generally believed to be affected by the physical and biochemical changes in the muscle which occurs during e.g. rigor mortis, freezing/thawing or processing. Water properties in muscle tissue have traditionally been assessed by measuring e.g. changes in total water content, water holding capacity (WHC), drip loss, and water activity. However, in recent years the non-invasive low-field NMR transversal (T_2) relaxation technique has been taken into use, examples of such studies are summarized in Chapter 5.

3.2.3 Lipids

Lean fish such as Atlantic cod (*Gadus morhua*) store lipids mainly in the liver, whereas fatty fish such as Atlantic salmon (*Salmo salar*) store lipids in fat cells distributed in other body tissues.

The white muscle of cod contains less than 1 % lipids. The lipid content of fatty fish varies considerably and is dependent on species, age, feed, season, etc. The variation in the percentage of fat is reflected in the percentage of water, since fat and water together make up around 80 % of the fillet. As a rule of thumb, this can be used to estimate the fat content from an analysis of the amount of water in the fillet (Katikou et al., 2001). The fatty fish species store lipids in fat cells throughout the body. Fat cells are typically located in subcutaneous tissue, in the belly flap muscle and in the white and red muscles. Fat depots are typically found spread throughout the muscle tissue structure. The concentration of fat cells appears to be highest close to the myocommata and in the region between the light and the dark muscle (Kiessling et al., 1991). **Figure 3** shows water and fat distribution of a salmon white muscle cube obtained by ^{1}H MR imaging.

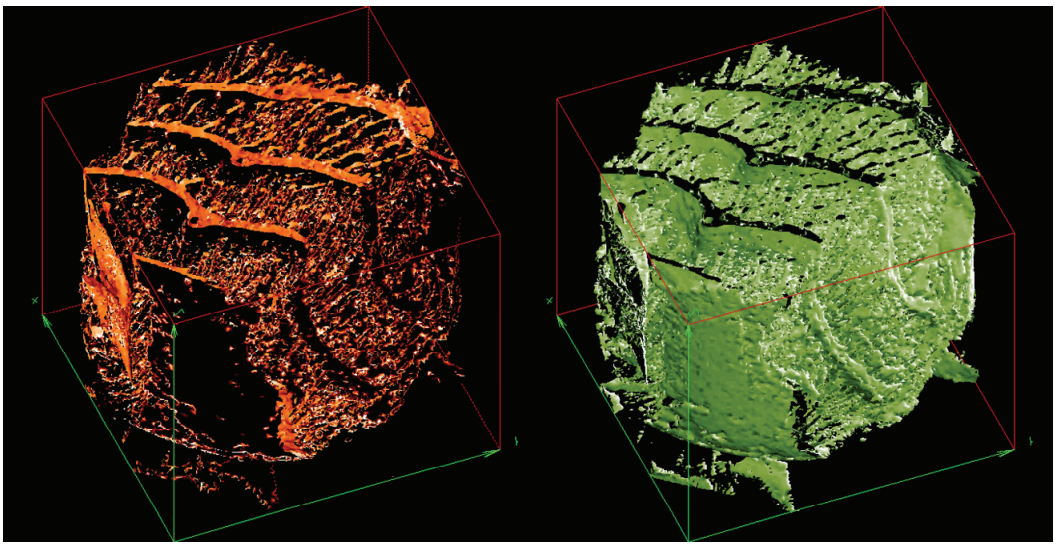

(A) (B)

Figure 3: Three dimensional ^{1}H MR imaging of an Atlantic salmon white muscle cube. (A) Fat and connective tissue and (B) water images based on ^{1}H MRI contrast (SINTEF Fisheries and Aquaculture, unpublished data).

Examples of the variation in muscle composition of cod, salmon, mackerel, herring and pork are given in **Table 1**.

Table 1: Proximate composition of edible muscle tissue from different species.

Species	Name	Chemical composition (%)				References
		Water	Protein	Lipid	Ash	
Atlantic cod	*Gadus morhua*	76-83	15.0-19.4	0.1-0.9	1	1-4
Atlantic salmon	*Salmo salar*	57-77	15.4-21.8	3.3-21.4	1-5	1-5
Mackerel	*Scomber scombrus*	60-74	16.0-20.0	1.0-23.5	-	2
Herring	*Clupea harengus*	60-80	16.0-19.0	0.4-22.0	-	2
Pork meat	*Musculus longissimus dorsi*	50-79	13.6-22.2	1.8-37	1.4	1, 4

[1]Watt and Merrill, 1963, [2]Murray and Burt, 1969, [3]Venugopal and Shahidi 1996, [4]NFSA, 2008, [5]NIFES, 2008

3.3 Post mortem changes

In live animals, contraction and relaxation of the striated muscle occurs by the sliding action of the thin actin filaments and the thick myosin filaments with the length of the filaments staying the same (Alberts et al., 1998). When muscle stimulation occurs, the myosin head interacts with actin resulting in a contraction forming actomyosin and using one molecule of ATP. Subsequently, the actin releases itself from the myosin and the muscle returns to its resting state. When the animal dies, the ATP-level gradually declines, and as a consequence action cannot be released from myosin. At this stage the muscle enters the state of rigor mortis (the conversion of muscle to meat starts). Simultaneously, muscle pH drops as glycogen degrades to lactic acid (Huff-Lonergan and Lonergan, 2005). As pH approaches the isoelectric point (pI) of the major proteins, especially myosin (pI = 5.4), the net charge of the protein becomes zero, meaning the number of positive and negative charges on the proteins are essentially equal. The positive and negative groups within the protein will attracted to each other, and the amount of water that can be held by that protein is reduced. Additionally, the repulsion between opposite charges within the myofibrillar protein ceases, allowing structures to pack more closely together. This, together with partial denaturation of myosin at low pH, results in a reduction of space within the myofibril (Offer, 1991; Huff-Lonergan and Lonergan, 2005).

The rigor process consists of an initial contractile phase (Tornberg et al., 2000), during which the muscle fibres contract, and a second stiff phase that is traditionally considered to be signified by a permanent binding of the contractile proteins myosin and actin. During the development of rigor, the diameter of muscle cells decreases (Hegarty, 1970; Swatland and Belfry, 1985) as a result of the lateral shrinkage of the myofibrils (Diesbourg et al., 1988). Additionally, during rigor development sarcomeres can shorten; which further reduces the space available for water within the myofibril. Honikel et al. (1986) showed that drip loss can increase linearly with a decrease in sarcomere length in muscle cells. Furthermore, Offer and Cousins (1992) found that a reduction in the muscle cell diameter occurred post mortem. Huff-Lonergan and Lonargan (2005) suggested that the rigor process could result in mobilization of water out not only out of the myofibril, but also out of the extramyofibril spaces as the overall volume of the cell is constricted. The sliding filament model of a muscle contraction is shown in **Figure 4**.

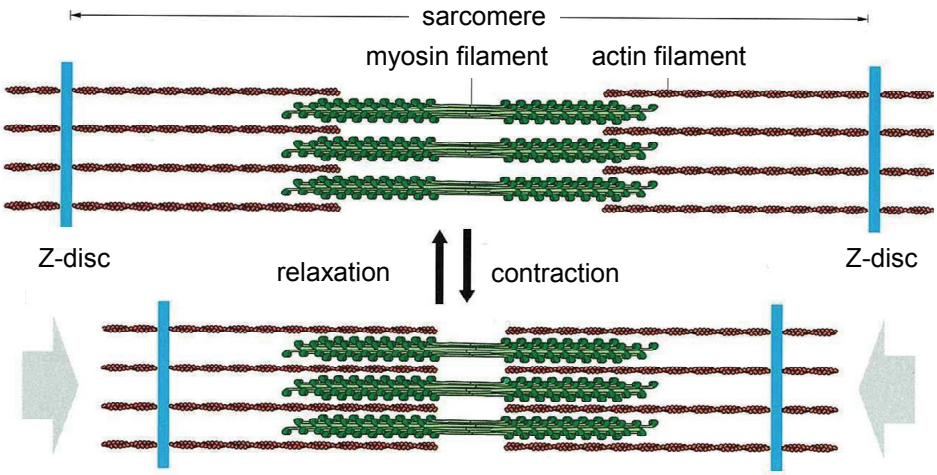

Figure 4: The sliding filament model of a muscle contraction. Upper panel: Relaxed muscle. Lower panel: During contraction, the actin and myosin filaments slide past each other (Alberts et al., 1998).

The water that is expelled from the myofibril and the muscle cell eventually gathers in the extracellular space. Several studies have shown that gaps develop between muscle cells and between muscle bundles during the post-rigor period (Offer et al., 1989; Offer and Cousins, 1992). **Figure 5** shows micrographs of the transverse sections of Atlantic salmon muscle pre and post rigor. A beginning widening of the extracellular matrix typical for post-rigor muscle structure is seen (Paper IV).

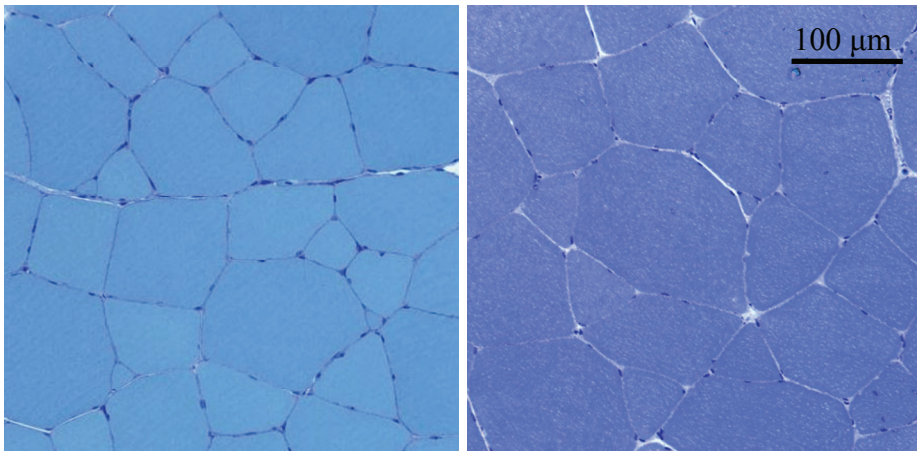

(A) (B)

Figure 5: Light micrographs of transverse sections of salmon muscle, sampled from the tail region of a fillet, (A) 3 h post mortem (pre rigor) and (B) 72 h post mortem (post rigor). A beginning widening of the extracellular matrix typical for post-rigor muscle structure is seen in the latter sample (Paper IV).

The location of water can be affected by changes in volume as the muscle undergoes rigor, leading to water being expelled from the intramyofibrillar space (Offer and Trinick, 1983). Consequently

one should expect a change in water mobility during the development of rigor mortis and in the post-rigor muscle.

3.3.1 Preslaughter conditions and development of rigor mortis

Present routines for the harvesting of Atlantic salmon commonly induce handling stress (excessive muscle activity) which in turn will shorten the time to onset of rigor mortis. In exhausted salmon, rigor onset typically occurs after 2 to 4 h post mortem (Erikson, 2001; 2008). If antemortem stress is avoided altogether, rigor onset is delayed for another 20 to 25 h (Erikson, 2001), and processing of in rigor fish can more easily be avoided. Ante-mortem stressed fish may develop stronger rigor mortis compared to rested harvested fish (Nakayama et al., 1992). This may also affect quality attributes such as fillet texture and water binding (Robb et al., 2000; Kiessling et al., 2004; Paper III). **Figure 6** shows typical rigor development for Atlantic salmon exposed to two extremes of ante-mortem handling; excessive stress until exhaustion and anaesthetization.

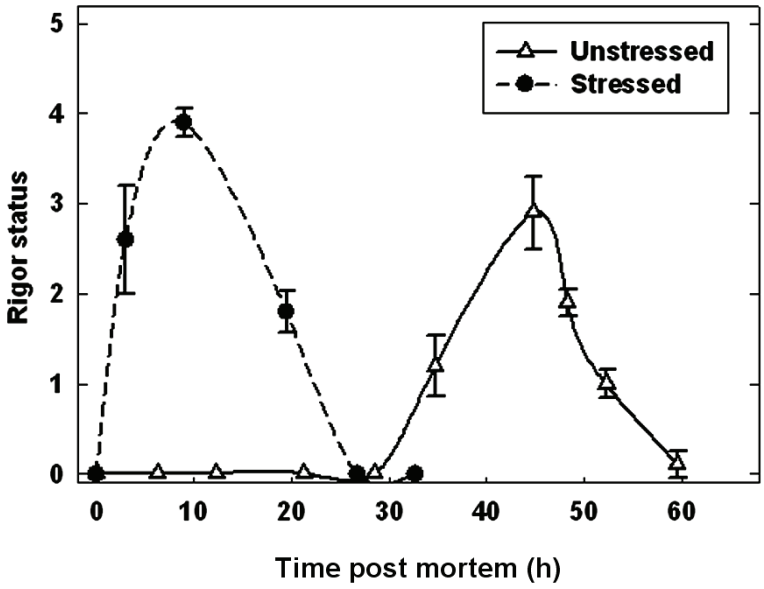

Figure 6: Development of rigor mortis of anaesthetized and exhausted Atlantic salmon during ice storage. Mean ± SD (n=25) (Misimi et al., 2008).

The concept of pre-rigor filleting is currently a goal for several salmon processors in Norway. To achieve this, it is essential to avoid preslaughter stress since this can delay the rigor onset. Pre-rigor fillets have several properties that differ from their post-rigor counterparts (Sørensen et al., 1997; Rørå et al., 2004; Kristoffersen et al., 2006). Mostly, these properties are considered favourable in terms of flesh quality (Skjervold et al., 2001a;b; Stien et al., 2005).

3.4 Processing

3.4.1 *Freezing*

Freezing is an important method in preserving and storing of fish products. During the freezing process, free water is transformed into ice crystals which cause mechanical damage to the muscle cell structure. Frozen storage gives rise to mechanical damage through ice crystal formation (Bello et al., 1982; Ayala et al., 2005) and protein denaturation (Fennema, 1990). As the structure of the meat is altered, properties including water holding capacity are affected (Ngapo *et. al*, 1999), which may have an impact on final product quality (Sigurgisladottir et al., 2000). A light micrograph of the transverse section of a salmon muscle before and after freezing and thawing is shown in **Figure 7**. An evident widening of the extracellular matrix is seen for the frozen/thawed muscle indicating muscle degradation as a function of freeze-damage.

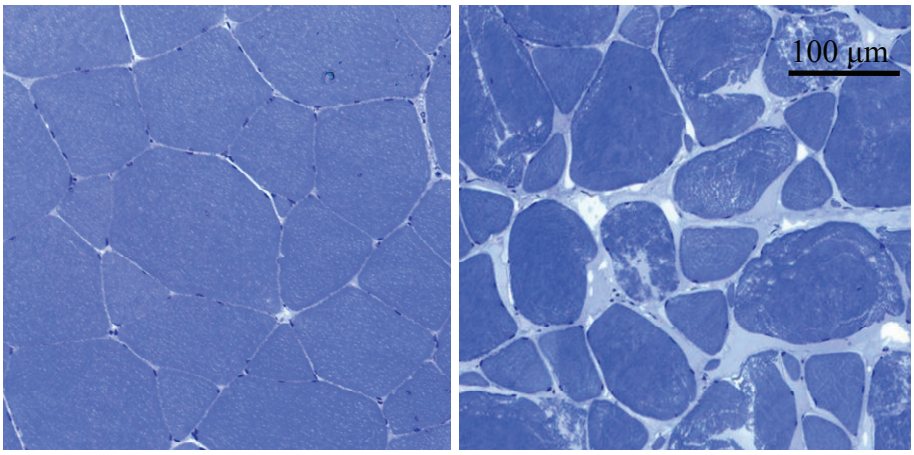

(A) (B)

Figure 7: Light micrographs of transverse sections of salmon muscle, sampled from the tail region of a fillet (A) post-rigor (3 days post mortem) and (B) frozen/thawed (Paper IV).

3.4.2 *Heating*

Meat undergoes considerable structural changes upon heating both regarding microstructure and protein structure. Response to thermal treatment depends on species, post-mortem aging, pH and ionic strength (Wright and Wilding, 1984; Offer et al., 1989; Fennema, 1990). An extensive review of the effects of heat on muscle proteins and its implications on structure and quality has been written by Tornberg (2005).

3.4.3 *Brine salting*

Since ancient times and up to now salting of muscle foods has been one of the most important food preservation methods. Addition of salt induces swelling of myofibers, a schematic illustration of the swelling is described by Offer et al., 1989 (**Figure 8**). Salt uptake resulting in swelling is coupled with an increase in water holding capacity (Hamm, 1960; Offer and Trinick, 1983; Offer and Knight, 1988a;b; Honikel, 1989). In meat tissue, salt (NaCl) contributes to water binding by expanding the filament lattice of myofibrils (Offer and Knight, 1988a;b) and by partially solubilizing the myofibrillar proteins (Hamm, 1986).

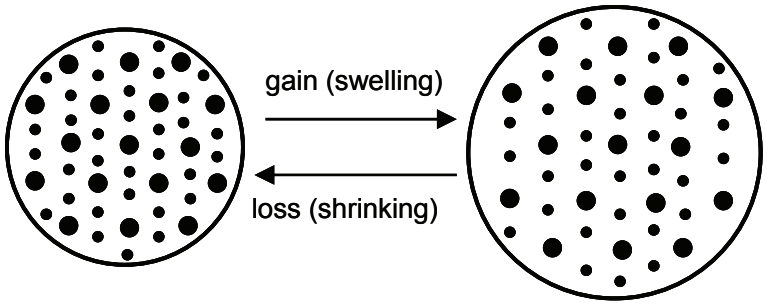

Figure 8: Illustration of myofiber swelling/shrinking due to water gain/loss (Offer et al., 1989).

Salting in brines leads to either water uptake or dehydration of the muscle depending on the brine concentration applied (Gallart-Jornet, 2007a). When salt molecules dissolve in water, a shell of bound water molecules is formed around the ions. As the concentration of salt increases, more and more water will be bound around the ions. This changes the water distribution in the tissue, and thereby most probably its mobility.

Addition of salt (NaCl) also influences the pH in the fish meat. When salt was added, the pH values of raw pork and beef decreased about 0.1 pH-units per %-unit of NaCl (Puolanne et al., 2001). When a neutral salt is added to an acidic solution, pH decreases linearly with increasing salt concentration provided the solution has no significant buffer capacity in the relevant pH range. In food the pH reduction will depend upon the buffer capacity of the food product, which can be substantial. Thus, it is not easy to predict the effect of adding salt in a product, except that pH will decrease. The effects of pH on meat quality have been thoroughly reviewed, e.g., by Hamm (1986), Bendall and Swatland (1988) and Offer and Knight (1988a;b).

4 Methodology

Nuclear magnetic resonance (NMR) opens up possibilities to study foodstuffs non-destructively and non-invasively. The technique was discovered independently by Bloch (Bloch et al., 1946) and Purcell (Purcell et al., 1946), for which they were given the Nobel prize in Physics in 1952. Since then, NMR has been applied to a wide variety of fields within many fields such as medicine, biology and food science. NMR-based methods have several advantages such as relatively rapid non-destructive and non-invasive measurements, and in some cases, a potential feasibility of being integrated into a process line. The use of NMR in the food science and industry has been extensively reviewed (Belton, 1990, Ruan and Chen, 2001; Hills, 1995; 1998). However, the use of NMR in food science is far from fully exploited, and lots of knowledge is still to be gained. Application of NMR methods in food research may be divided into three main groups according to the type of equipment used, which provide useful information about the chemical composition and structure of biological systems at various levels. These are: high-resolution NMR (HR NMR) spectroscopy, magnetic resonance imaging (MRI) and low-field NMR relaxometry. The two latter modalities have been applied in the work of the present thesis. The following chapter gives an introduction to the basic concept of NMR. The methodologies of low-field ^{1}H NMR and ^{1}H/^{23}Na MRI techniques are given a particular attention.

4.1 The principle of NMR

The NMR phenomenon is based on the fact that nuclei of atoms have magnetic properties that can be utilized to yield chemical information. From a quantum mechanical point of view subatomic particles (protons, neutrons and electrons) possess a property called nuclear spin. These spins can be paired in some atoms (e.g. ^{12}C, ^{16}O, ^{32}S), cancelling each other out so that the nucleus of the atom has no overall spin. However, in certain atoms the nucleus does possess an overall spin (^{1}H, ^{13}C, ^{31}P, ^{15}N, ^{19}F, ^{23}Na, etc.). Nucleus with a non-zero overall spin generates a magnetic moment. Like a normal magnet bar, this magnetic moment has a north and a south pole. When the nucleus possessing magnetic moment is placed in a static magnetic field, it will interact with this field resulting in a wobbling or angular spinning which is called nuclear precession. The frequency of this precession of the nucleus is called Larmor frequency defined by the Larmor equation;

$$\omega = -\gamma B_0 \qquad \text{(Eq 1)}$$

where ω is the frequency of precession, B_0, is the strength of the static magnetic field, and γ is termed the magnetogyric ratio (often named gyromagnetic ratio) and has a precise value characteristic for each nuclear species. Physically the magnetogyric ratio of a nucleus is the ratio of

its magnetic dipole moment to its angular momentum. Proton has a γ of 42.576 MHz/T and sodium has a γ of 11.262 MHz/T (Ruan and Chen, 2001).

According to quantum mechanical principles, the nuclear spins can only preceess around the direction either along or opposite to the static field B_0. Populations of the corresponding energy levels will be slightly different, and a small but detectable net magnetization along B_0 will be created. The frequency of the nuclear precessing ω_0 is typically in the radio frequency (RF) range (megahertz). Therefore, by using an RF coil operating at exactly the same frequency ω_0, one can transfer energy of the external RF radiation to the nuclei causing a resonant absorption. This phenomenon is called nuclear magnetic resonance (NMR). Having absorbed the extra energy, the nuclear system will no longer be in the energetic equilibrium and will re-emit RF radiation and return to the lower-energy state. This process is called spin-lattice relaxation and is characterized by a time constant, T_1. Spins taken out of the equilibrium at a certain time moment by an RF pulse will first precess coherently and there will be a non-zero component of the net magnetization in the plane transversal to B_0. The oscillating at the resonance frequency magnetic field will induce current in the same RF coil, which can be detected as an NMR signal. Small differences in the precessing frequency in the ensemble of nuclei will cause loss of the transversal coherence, a process called spin-spin relaxation or transversal relaxation with its characteristic time T_2.

4.2 NMR relaxometry

Whereas longitudinal (T_1) relaxation causes a loss of energy from the spins, transverse (T_2) relaxation occurs by a mutual swapping of energy between spins, i.e. longitudinal relaxation is thus an enthalpic process whereas transverse relaxation is entropic.

T_2 is proportional to the rate of rotational motion of the molecules. A larger T_2 generally means greater mobility. T_2 relaxation is affected by a chemical exchange process, which is especially true in muscle food systems. Chemical exchange takes place between different sites of different mobilities. Protons of water exchange with protons of macromolecules, and protons of more mobile water exchange with protons of less mobile water molecules, etc. The rate of exchange has great influence on the T_2 value. If the exchange is very fast, the difference in T_2 of the two exchanging sites is averaged. On the other hand, if the exchange rate is low, a broad distribution of T_2 or several separate T_2 compartments can be expected. While the proton intensity is related to the concentration of proton-containing compounds in foods, relaxation times provide information about the motional properties of food systems. The most widely used pulse experiment for determination of T_2 is the

Carr-Purcell-Meiboom-Gill (CPMG) sequence (Carr and Purcell, 1954; Meiboom and Gill, 1958) shown in **Figure 9**. A good introduction to NMR spectroscopy was written by Farrar (1987).

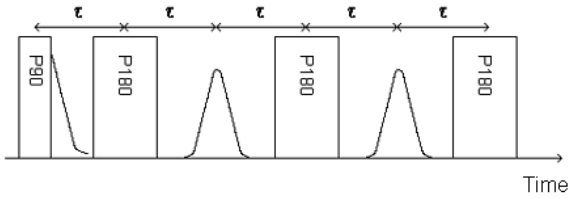

Figure 9: CPMG pulse sequence.

4.3 Low-field NMR

Low-field NMR (often also called time-domain NMR) is a fast and powerful method that can be used for non-invasive determination of water and fat content as well as to study water and fat mobility in e.g. muscle foods. The application of low-field ^{1}H NMR to fish and fish products opens up a possibility to relate the state and dynamics of water to various technological parameters, such as raw material quality, storage and processing conditions. Furthermore, the structure of muscles can be studied indirectly using low-field ^{1}H NMR. Different tissue water populations can be studied because protons in different environments exhibit different T_2 relaxation properties. Different approaches exist to extract useful information from raw CPMG curves. In the following, an overview of the data analysis methods used in this thesis is given.

4.3.1 Low-field NMR T_2 relaxation data analysis

In general a T_2 relaxation curve from an object containing N relaxation populations can be mathematically described by a sum of N discrete exponential functions given by;

$$S(t) = \sum_{i=1}^{N} A_i e^{-\frac{t}{T_{2i}}} \qquad \text{(Eq 2)}$$

where $S(t)$ is the recorded CPMG signal, A_{2i} is a partial amplitude of the i-th relaxation component present in the curve and T_{2i} is its corresponding relaxation time.

In fish tissue a limited number of components have been identified in fresh (Andersen and Rinnan; 2002; Jepsen et al.; 1999), frozen/thawed, chilled and processed (Lillford et al.; 1980; Steen and Lambelet, 1997; Løje et al., 2007; Jensen et al., 2002; Lambelet et al., 1995) tissue and mince. In order to extract information from the relaxation curves several methods are available, each with their own strengths and weaknesses. The methods may be classified into single sample algorithms and multivariate data analysis. In the work of this thesis four different methods were combined.

The classical way of extracting information from relaxation curves is by *exponential curve fitting.* This is a single sample algorithm based on a predefined assumption of the number of components in the data set. This simple and robust method has traditionally been used to interpret T_2 relaxation data. However, one should remember that this form of data processing forces the curve to be fitted by a chosen number of exponentials. Therefore, it is important to thoroughly investigate the residuals of the exponential fittings, to make sure that the right number of exponents is chosen. A general rule is to find a minimal number of exponentials satisfactorily describing the experimental curve, such that additional exponents would not substantially improve the fit. In fish, two (biexponential) or three (triexponential) exponents are usually chosen (Eq 3 and Eq 4, respectively). Denote the signal amplitude S_i, where i is the number of exponential terms. Then, the biexponential and triexponential functions describing signal strength may be written as:

$$S_2 = A_1 e^{-t/T_{21}} + A_2 e^{-t/T_{22}} \qquad \text{(Eq 3)}$$

$$S_3 = A_1 e^{-t/T_{21}} + A_2 e^{-t/T_{22}} + A_3 e^{-t/T_{23}} \qquad \text{(Eq 4)}$$

Figure 10 shows typical residuals for mono-, bi- and triexponential curve fittings of T_2 relaxation data obtained on raw post-rigor Atlantic salmon (*Salmo salar*). The residuals are normalized with respect to the number of echoes. Approximately the same residual values were obtained for two and three exponents. This indicates that the main information stored in the data set is described by two components, i.e. the larger part of the tissue water is described by two main populations.

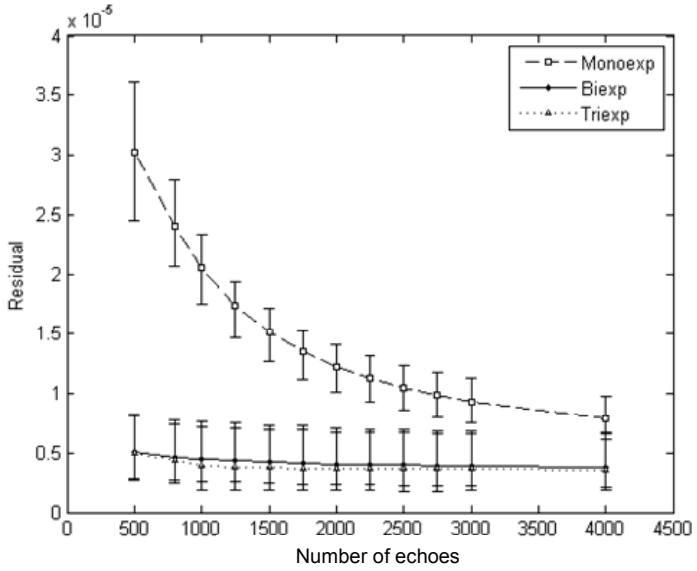

Figure 10: Normalized residuals of mono-, bi- and three exponential fitting to varying number of echoes (500 – 4000) of T_2 relaxation curves obtained on post-mortem Atlantic salmon muscle exposed to ante-mortem stress (n=6). Mean ± max/min.

Another single sample algorithm to extract information from the T_2 data is *inverse Laplace transformation*. A commonly used implementation is the computer algorithm called CONTIN developed by Provencher (1982). This involves an iterative optimization-based search algorithm. Assume that the T_2 signal *S(t)* is represented by Eq 2. Then, the Laplace transformation *F(s)* may be written:

$$F(s) = \int_0^\infty S(t)e^{-st}dt \qquad \text{(Eq 5)}$$

The method gives an overview of the characteristics of the different water populations in the studied samples. The Inverse Laplace Transformation (ILT) is a highly ill-posed problem and is therefore intrinsically affected by numerical instability. The CONTIN algorithm searches for a *F(s)* that fits the recorded *S(t)*. Data sets obtained from the experiments are affected by some noise, and this will have influence on the search algorithm. Numerical differentiation is involved in a regularization process during the search, and this is an operation very sensitive to noise. Thus, one should apply this algorithm with care. Its solution may not be unique, may not exist or may not depend continuously on the data. The output of the algorithm is only one of the possible solutions, and this limitation is unavoidable. Changing the parameters, the solution may change too. Despite these challenges, the use of ILT may be really successful if used together with other methods like for instance traditional exponential fitting. The latter results can be used to choose reasonable guess values for the inverse Laplace transformation calculations, and thereby give a more reliable convergence. Furthermore, noise may be reduced by low-pass filtering of the relaxation signal *S(t)*, providing a more robust input to the optimization search necessary for ILT estimates. Although such use of related methods will give dependency between results obtained by Inverse Laplace transformation and exponential curve fitting, the results are found to be important to support and elaborate the information found in the data set. In that way, more reliable results can be achieved.

Multivariate data analysis is another way of treating the relaxation data. By making use of the full data set from several samples at the same time, new possibilities arise. *Principal component analysis (PCA)* (Jolliffe, 1997; Martens and Martens, 2001) aims at reducing a large number of variables in the data matrix *X*, to a smaller number of uncorrelated "latent" variables or principal components (PCs). The PCs comprise linear combinations of the original variables. The first PC accounts for the main variation, while the second PC contains second most variation. That is, each new variable that follows, explains as much of the remaining variation as possible (Næs et al.,

2002). The method is robust and rapid and can be performed directly on the raw T_2 relaxation curves to investigate differences between sample groups etc. *Partial least square regression* (PLSR) is a multivariate statistical method that attempts to find the relationships between two matrices *X* and *Y*. The *X* matrix can i.e. consist of T_2 relaxation curves and the *Y* matrix of physico-chemical data. Like in PCA, the guiding principle for PLSR is a decomposition of the *X* matrix into scores and loadings. However, in PLSR the decomposition is governed by the variables of the *Y* matrix. In PLSR the response variables *Y* are expressed as a linear function of the variables;

$$Y = B_0 + XB + F \qquad \text{(Eq 6)}$$

where B_0 is the matrix of offsets with identical values in every column, *B* is the matrix of regression coefficients and *F* the matrix o residuals (Martens and Martens, 2001).The directions in this new co-ordinate space are given by the loading vectors and the new variables are ordered according to the magnitude of their co-variance to *Y*. The first PLS component contains the largest co-variance, the second PLS component has the second largest variation, and so forth (Næs et al., 2002). PLSR can be used for prediction of quality parameters, without having to pre process the raw relaxation curves to extract specific relaxation components explicitly. The technique has e.g. been applied in the determination of sensory attributes of potatoes (Thybo et al., 2000; Thygesen et al., 2001) The PCA and PLSR techniques are useful in the investigation of differences between groups, the location of potential outliers, or e.g. as a basis for calibration models in determination of quality parameters. However, these calculations can not directly extract T_2 relaxation components.

Table 2 gives a summary of the T_2 relaxation data analysis methods used in the work of this thesis, their advantages and disadvantages.

Table 2: Low-field ^{1}H NMR T_2 relaxation data analysis methods, their advantages and disadvantages.

Data analysis method	Advantage	Disadvantage
Single sample algorithms		
Exponential fitting	T_2 relaxation times and populations can be calculated. Classical robust method. Easy to compare results with data in literature.	Risk of overfitting, close investigation of residual is essential.
Continuous distributed curve fitting / Inverse Laplace transformation	T_2 relaxation times and populations can be calculated. Results in a curve from which N is directly determined as the number of peaks. Dynamic changes in relaxation populations are easy to follow.	Highly affected by numerical instability.
Multivariate data analysis		
Principal Component Analysis (PCA)	Robust and rapid method. Good tool for building calibration models. Good performer when linear relationships are present. Most of the original variance is captured in a few principal components. Allows detection of underlying patterns and trends.	Sensitive to outliers in the data set. Can be hard to interpret the PCs. T_2 relaxation times and populations can not be directly calculated.
Partial Least Squares Regression (PLSR)	Good tool for building calibration models. Can be used for prediction of quality parameters. Calibrations are generally robust provided that calibration set accurately reflects range of variability expected in unknown samples.	Sensitive to outliers in the data set. Models are more abstract, thus more difficult to understand and interpret. Generally, a large number of samples are required for accurate calibration. T_2 relaxation times and populations can not be directly calculated.

4.4 MR imaging

MR imaging (MRI) is an extension of NMR. It provides additional spatial information about nuclear spins in the investigated object. The first published MR image is credited to Paul Lauterbur (1973). As a research tool, MRI can give us basic insight into i.e. structure of tissues as well as distribution of fat and water. MRI can also be used as a tool in the optimization of various processes such as freezing-thawing and salting (Hills, 1998).

4.4.1 ^{1}H MR imaging

The fact that water and lipid distributions can be imaged non-invasively accounts for the impact that MRI has had in medical diagnosis. Similar anatomical details are important when monitoring the physiological changes in muscle foods. For instance, differences in fat distribution in the flesh of brown trout due to low- or high-energy diets have been demonstrated by using MRI (Toussaint et al., 2005). Furthermore, it is possible to produce 'diffusion weighted' MR images showing only molecules with low mobility (Mulkern and Spencer, 1988) or high-resolution images of connective tissue (Bonny et al., 2001). MRI methods based on double-quantum filtering can suppress the signal from isotropic fluids and only detect molecules associated with ordered tissue structures (Tsoref et al., 1998). An overview of different fat and water selective MRI techniques was written by Tingle et al. (1995).

4.4.2 ^{23}Na MR imaging

The distribution of salt (NaCl) in the fish tissue during salting is important, partly because a homogeneous distribution in the final product is desired. It is also important in the development of salting procedures and in the choice of salting technique. Numerous studies have been performed on the salting of foods by using standard physicochemical methods. Investigations of the stability, degradation, or denaturation of muscle proteins (Duerr and Dyer, 1952; Thorarinsdottir et al., 2002; Martínez-Álvarez and Gomez-Guillen, 2005; Sannaveerappa et al., 2004), effects of additives and salting procedure (Jittinandana et al., 2002; Thorarisdottir et al., 2004; Esaiassen et al., 2005), process modelling and mass transfer kinetics (Wang et al., 1998; Wang et al., 2000; Barat et al., 2002; Barat et al.; 2003; Gallart-Jornet et al., 2007a;b), as well as raw material quality (Rørå et al., 1999; Lauritzen et al., 2004) have been made. Common features of all these techniques were that they were destructive for the sample. ^{23}Na MRI, however, can be used to non-destructively visualize variations in the sodium distribution of similar raw materials salted or processed by different methods, and thus serve as a tool for the process optimization. Moreover, theoretical

transport models can in turn be used to interpret the images. This technique has earlier been used to study i.e. salting and desalting of cod (Erikson et al., 2004), and the salting process of cod (Gallart-Jornet et al., 2007b) and salmon (Foucat et al., 2006; Gallart-Jornet et al., 2007b).

4.5 Instrumentation

Low-field NMR instruments are based on use of permanent magnets covering a range of proton resonance frequencies from about 2 to 60 MHz. Magnet bore openings of typical low-field NMR equipment range from 5 to 52 mm in diameter. Furthermore, a single-sided NMR instrument, Bruker ProFiler, has been developed. This is a low-field mobile NMR analyzer for near-surface volume measurements of samples unrestricted in size. A basic diagram of a typical low-field NMR instrument is shown in **Figure 11**. The main advantages of the low-field NMR method compared with the other NMR techniques are low investment costs, small size, no maintenance costs (permanent magnet), excellent stability, high degree of automation and easy operation. Low-field NMR can be implemented at-line to operate under rather harsh industrial conditions.

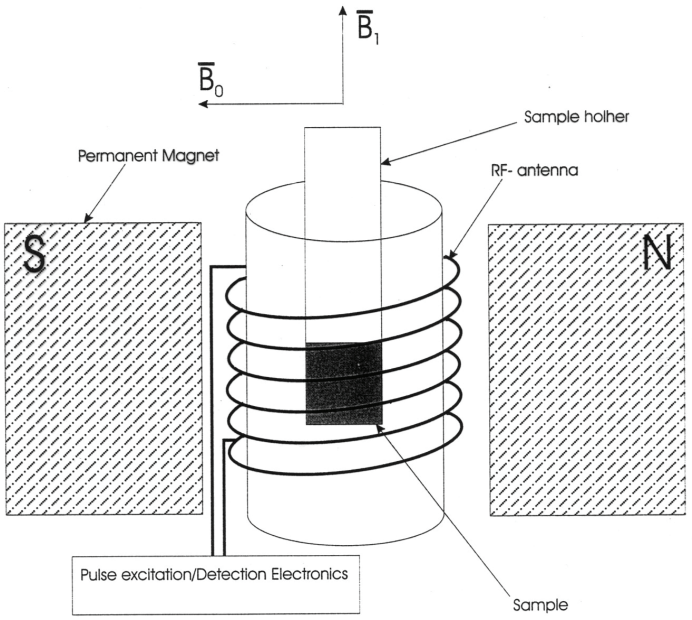

Figure 11: NMR instrument.

A typical MRI scanner consists of the following main elements; a superconducting magnet generating a static magnetic field, an RF coil used to transmit radio-frequency excitation into the material to be imaged. Gradient coils are used to spatially encode the positions of protons by varying the magnetic field linearly across the imaging volume. This excites a component of magnetization in the transverse plane which can be detected by the same RF coil or a separate

reception coil. The signals are transduced and conditioned prior to image reconstruction. A basic block diagram of a typical MRI data-acquisition system is shown in **Figure 12**. Current MRI scanners generate images with sub-millimetre resolution of virtual slices through the sample. The thickness of the slices is often of a millimetre, although thicker slices can be imaged in special cases. Contrast resolution between materials depends strongly on the strength of the magnetization, T_1, T_2, and movement of the nuclei during imaging sequences.

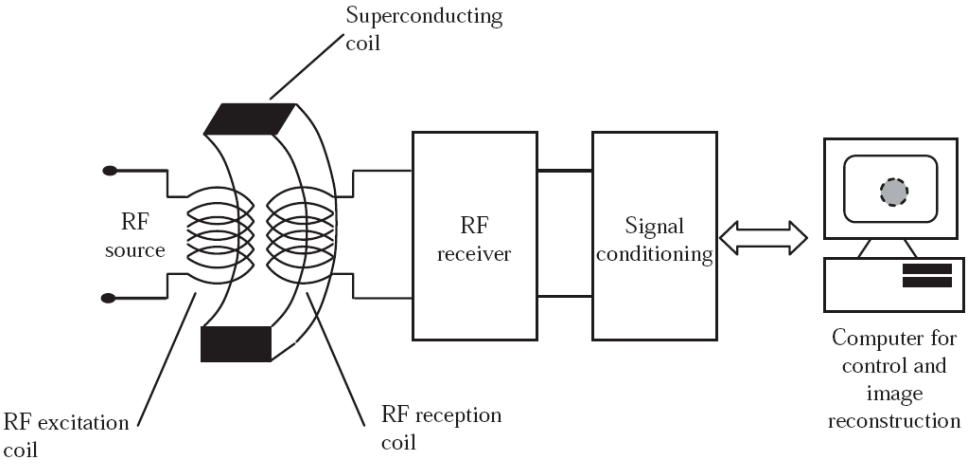

Figure 12: A block diagram of a typical MRI data-acquisition system (Sun and Zheng, 2007).

Due to the high investment costs, often small magnet bore opening, the requirement of trained personnel and the necessary related infrastructure, MRI is not a standard measuring technique in the food industry. However, the rapidly decreasing cost of electronic components, combined with the increasing need for innovation in the food industry, indicate that in the future, MR imaging may be used for food quality control industrially. In fact, instruments have already been implemented in the baby-food industry for quality control of the final product (Hills, 1998). However, today, these types of instruments have their main advantages as a research tools.

The low-field NMR and the MRI instruments applied in the present thesis are shown in **Figure 13**, and instrumental details are given in **Table 3**.

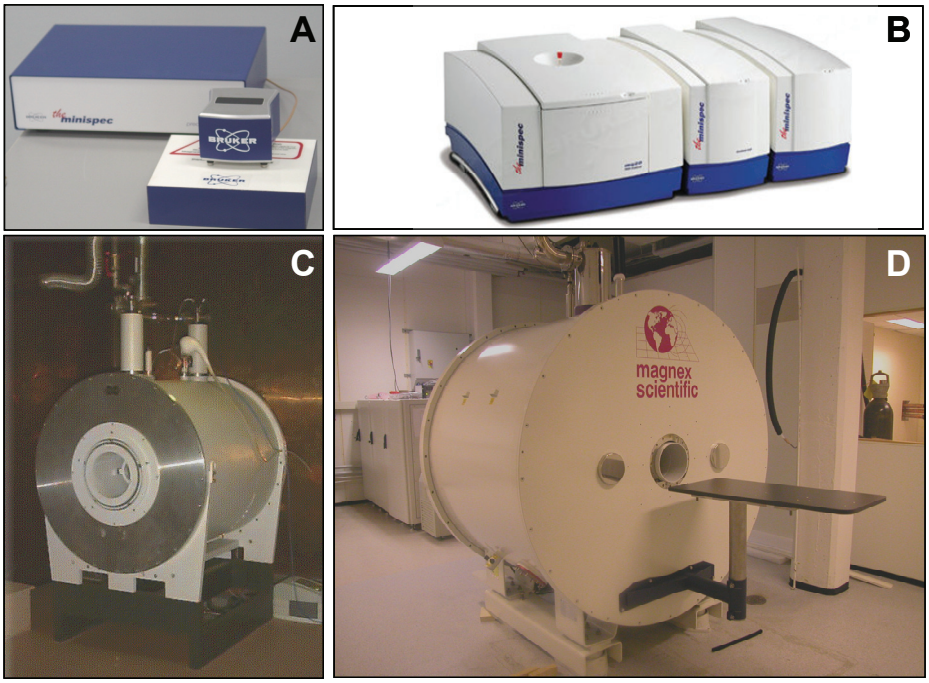

Figure 13: Picture of the low-field NMR and MR imaging instruments used in the research of the present thesis (A) low-field NMR surface scanner, (B) low-field NMR bench top instrument, (C) 100 MHz MRI instrument, (D) 300 MHz MRI instrument. Technical details are given in **Table 3**.

Table 3: Instruments and probes/coils used in the work of this thesis.

Instrument	Technical characteristics	Probes/Coils
Bruker ProFiler	Highly inhomogeneous magnetic field with a constant gradient in the order of 10 T/m at the surface. Measuring volume about 5×5 mm in-plane and 2.5 mm in-depth	Surface probe
Bruker minispec mq 20	20 MHz ^{1}H spectrometer equipped with: - 225 W power amplifier - Quadrature detection receiver system - 12 bit ADC (1 MHz) - 1 axis gradient z (2 T/meter)	- 10 mm coil with z-gradient for diffusion measurement. - Variable temperature in the range -70 to +200 ºC.
Bruker Avance DBX 100, Biospec	100 MHz ^{1}H multinuclear spectrometer equipped with: - 2 broad banded 1 KW power amplifier - 3 axis gradient controller - 2 gradient coil sets, 200 mT/meter, and 50 mT/meter - Quadrature detection receiving system, 16 bit HR ADC and 12 bit FAST ADC	- ^{1}H birdcage coil (200 mm) - ^{1}H birdcage coil (70 mm) - In-house made ^{23}Na probe (70 mm)
Bruker Avance AV 300, 7 T small animal magnet	System: 300 MHz ^{1}H multinuclear spectrometer equipped with: - 2 broad banded 500 W power amplifier - 1 KW power amplifier - gradient coil set, 400 mT/meter - Quadrature detection receiving system, 16 bit FAST ADC	- ^{1}H Birdcage coil (72 mm) - ^{1}H/^{23}Na double tuned birdcage coil (72 mm)

5 Low-field NMR and MRI studies on fish

This chapter summarizes examples of applications of low-field NMR and MRI on fish tissue. **Table 4** gives an overview of application examples including the contributions of the present thesis.

Table 4: Overview of fish application using low-field (LF) NMR and MRI.

Application	NMR method	Fish species	Reference
Raw material characteristics			
Distinguishing organs	^{1}H MRI	Embryonic fish	Blackband and Stockopf, 1990
Blood flow	^{1}H MRI	Eelpout (*Zoarces viviparous*) Atlantic cod (*Gadus morhua*) in vivo studies	Bock et al., 2002
Anatomical defects	^{1}H MRI	Atlantic salmon (*Salmo salar*)	Veliyulin et al., 2006a
Fat and collagen distribution	^{1}H MRI	Frozen-thawed rainbow trout (*Salmo gairdneri*)	Nott et al., 1999b
Fat distribution	^{1}H MRI		Collewet et al, 2001
Water and fat distribution	^{1}H MRI	Atlantic salmon (*Salmo salar*)	Veliyulin et al., 2006a
Water and sodium distribution	^{1}H/^{23}Na MRI	Atlantic cod (*Gadus morhua*)	Veliyulin et al., 2006a
Fat content and distribution	LF NMR and ^{1}H MRI	Atlantic salmon (*Salmo salar*)	Paper II
Liver fat content	^{1}H MRI	Live burbot (*Lota lota*)	Alanen et al, 1991
Fat and water content	LF NMR	Salmon	Bechmann, et al., 1998
Fat and water content	LF NMR	Atlantic salmon (*Salmo salar*) Atlantic cod (*Gadus morhua*)	Jepsen et al., 1999
Fat content	LF NMR	Brown trout (*Salmo trutta*)	Toussaint et al., 2001
Fat content	LF NMR ProFiler	Live Atlantic salmon (*Salmo salar*)	Veliyulin et al, 2005
Fat content	LF NMR	Herring (*Clupea harengus L*)	Nielsen et al., 2005
Fat content	LF NMR mobile surface scanner	Atlantic salmon (*Salmo salar*)	Paper I
Fat and water content	LF NMR	Atlantic salmon (*Salmo salar*)	Paper I
Preslaugher handling stress	LF NMR and ^{1}H/^{23}Na MRI	Atlantic salmon (*Salmo salar*)	Paper III
Rigor status	LF NMR and ^{1}H/^{23}Na MRI	Atlantic salmon (*Salmo salar*)	Paper IV
Quality attributes			
Texture during frozen storage	LF NMR	Frozen mince of Atlantic cod	Steen and Lambelet, 1997
WHC	LF NMR	Atlantic salmon (*Salmo salar*) Atlantic cod (*Gadus morhua*)	Jepsen et al., 1999
Water content and distribution	LF NMR	Atlantic cod (*Gadus morhua*)	Andersen and Rinnan, 2002
WHC	LF NMR	Atlantic cod (*Gadus morhua*)	Andersen and Jørgensen, 2004
Water distribution Seasonal variation	LF NMR	Herring (*Clupea harengus*)	Jensen et al., 2005

Table 4 continued: Overview of fish application using low-field (LF) NMR and MRI.

Application	NMR method	Fish species	Reference
Changes during processing and storage			
Salting and desalting	LF NMR and $^{1}H/^{23}Na$ MRI	Atlantic cod	Erikson et al., 2004
Salting	^{1}H /^{23}Na MRI	Atlantic salmon (*Salmo salar*)	Foucat et al., 2006
Brine salting	$^{1}H/^{23}Na$ MRI	Atlantic cod (*Gadus morhua*) Atlantic salmon (*Salmo salar*	Gallart-Jornet et al., 2007b
Brine salting, sodium MRI visibility	$^{1}H/^{23}Na$ MRI	Atlantic cod (*Gadus morhua*) Atlantic salmon (*Salmo salar*)	Veliyulin and Aursand, 2007
Smoking	LF NMR	Atlantic salmon	Løje et al., 2007
Brine salting	LF NMR and $^{1}H/^{23}Na$ MRI	Atlantic salmon (*Salmo salar*)	Paper III and Paper IV
Brine salting	LF NMR	Atlantic cod (*Gadus morhua*) Atlantic salmon (*Salmo salar*)	Paper V
Frozen storage Heating Pressure treatment	LF NMR	Atlantic cod (*Gadus morhua*)	Lambelet et al., 1995
Frozen storage	^{1}H MRI	Atlantic cod (*Gadus morhua*)	Howell et al., 1996
Frozen storage	^{1}H MRI	Atlantic cod (*Gadus morhua*) Mackerel (*Scomber scombrus*)	Nott et al., 1999a
Frozen storage	^{1}H MRI	Trout	Foucat et al., 2001
Frozen storage and chilled storage (MAP)	LF NMR	Atlantic cod (*Gadus morhua*)	Jensen et al., 2002
Freezing	^{1}H MRI	Atlantic salmon (*Salmo salar*)	Veliyulin et al., 2006a
Frozen storage	LF NMR	Atlantic salmon (*Salmo salar*)	Paper II
Frozen storage	LF NMR and $^{1}H/^{23}Na$ MRI	Atlantic salmon (*Salmo salar*)	Paper IV

Low-field NMR and MRI have also been applied in the study of meat. Low-field NMR has been used for the determination of water holding capacity (Renou et al., 1985a, Tornberg et al., 1993; Brøndum et al., 2000; Brown et al., 2000,; Bertram et al., 2001a) and for the determination of fat content (Renou et al., 1985b; Pedersen et al., 2001). Furthermore, the technique was used for studying the conversion of muscle to meat (the rigor process) (Bertram et al., 2002a; b), cooking (Micklander et al., 2002; Bertram et al., 2004), and freezing/thawing (Yano et al., 2002). MR imaging has been applied to meat to estimate whole carcass composition (Mitchell et al., 1991; Scholz et al., 1995) and muscle/meat composition (Bonny et al., 2001; Ballerini et al., 2002). Furthermore, sodium MRI has been used in the study of meat curing (Foucat et al., 1995; Guiheneuf et al., 1995; Guiheneuf et al., 1996) and freezing/thawing (Guiheneuf et al., 1997; Hall et al., 1998; Kerr et al., 1998).

6 Main results and discussion

The results of this thesis are enclosed in Part 2. In this chapter, a short summary of the obtained results is given. Furthermore, the relevance for fish research and industry is discussed.

6.1 Non-destructive water and fat determination

Low-field NMR methods for rapid determination of water and fat have earlier been developed for different foodstuffs (**Table 4**). However, we wanted to build a calibration model for rapid determination of fat and water in Atlantic salmon muscle. Moreover, we wanted to investigate the applicability of the single sided NMR ProFiler (sometimes referred to as NMR mouse) for rapid determination of fat. Both methods proved to be rapid and accurate (Paper I). A similar approach developed at SINTEF (Veliyulin et al., 2006b) has been successfully implemented at-line with one of the largest Norwegian fish feed companies. For the fish processing industry, an on-line application would be preferable. However, there are still some practical concerns to be concidered before NMR technology can be integrated into a fish processing line (Hills, 1998; Ruan and Chen, 2001). For instance, one needs custom made magnets tailored to the size of fish. Inherent low sensitivity of the NMR technique imposes certain problems on the speed of the NMR measurement (a Norwegian salmon processing plant typically slaughter 100 - 150 tons of fish a day, and the speed of measurements should at least be 1 fish/sec). Furthermore, other measuring techniques such as NIR are already implemented on-line in the salmon processing industry for fat measurements. However, on-line implementation of NMR in the fish processing industry might happen in the future.

Proton MRI has been applied to many kinds of seafoods (**Table 4**) e.g. to investigate the distribution of fat and water in the tissue. In Paper II, MR images of water and fat separately was obtained based on a chemical shift selective (CHESS) imaging protocol. Quantification of fat and water in the images gave good correlation with values obtained by chemical analysis. Information about spatial fat and water distribution is important factors especially in the optimization of processing such as salting.

6.2 T_2 relaxation - Tissue water dynamics

The number of T_2 populations reflecting tissue water is a topic of discussion. In fish and meat, two components, T_{21} and T_{22}, with relaxation times of 35-50 ms and 100-250 ms, respectively, are often reported (Tornberg, 1993; Lambelet et al., 1995; Erikson et al., 2004). These two relaxation

components represent 80-95% and 5-15% of the relaxation, respectively (Tornberg, 1993). Other studies report three (Steen and Lambelet, 1997) or four components (Jensen et al., 2002). Studies on pork (Bertram et al., 2002b) have reported three peaks thought to reflect protein bound (T_{2b}), intramyofibrillar (T_{21}) and extramyofibrillar (T_{22}) water, respectively. The work of this thesis does not aim at investigating the exact number of water populations, but rather to examine the changes in the main water populations in fish flesh, since this water is known to be determining for functional properties such as e.g. water holding capacity and drip loss of tissues. A summary of the obtained changes in T_2 relaxation as affected by raw material quality and fish processing are shown in the following paragraphs.

6.3 Spatial fat distribution and T_2 relaxation

Many T_2 relaxation studies on fish have been performed on lean species such as Atlantic cod. However, when working with fatty tissues one must remember that both water and fat protons give rise to the NMR T_2 relaxation signal. In the study of water dynamics of fatty tissues it is important to have a clear picture of the relaxation behaviour of fat. In Paper I and Paper II, two-dimensional diffusion weighted T_2 relaxation experiments were performed. By use of this technique, we were able to separate fat and water into distinct populations. It was found that in Atlantic salmon tissue, both fat and parts of the tissue water is reflected by the T_{22} component.

6.4 Tissue microstructure and T_2 relaxation

The relationship between tissue structure and T_2 relaxation has mainly been studied on meat. It has been suggested that transverse relaxation reflects structural features of the material, as the relaxation rate will depend on the probability of a water molecule to meet a surface and thereby also the anatomical features (Lillford et al., 1980). Later on, Bertram et al. (2002b), who studied pork muscle, found correlations between the T_{21} relaxation time and the sarcomere length. Studies investigating the relationship between fish tissue microstructure and the T_2 relaxation have not been reported earlier. In Paper IV different Atlantic salmon tissue microstructures were designed by controlling the rigor status of the samples (pre and post), by freezing/thawing and by brine salting. The study revealed that T_2 relaxation is linked to changes in tissue microstructure as affected by rigor status, freeze-thawing and salt-induced swelling. An example of how the differences in microstructure can be observed by T_2 relaxation is seen in **Figure 14.** A shift towards longer T_{21} relaxation times and larger T_{21} populations (Paper IV) were coupled to the salt-induced swelling of myofibers in frozen/thawed salmon tissue.

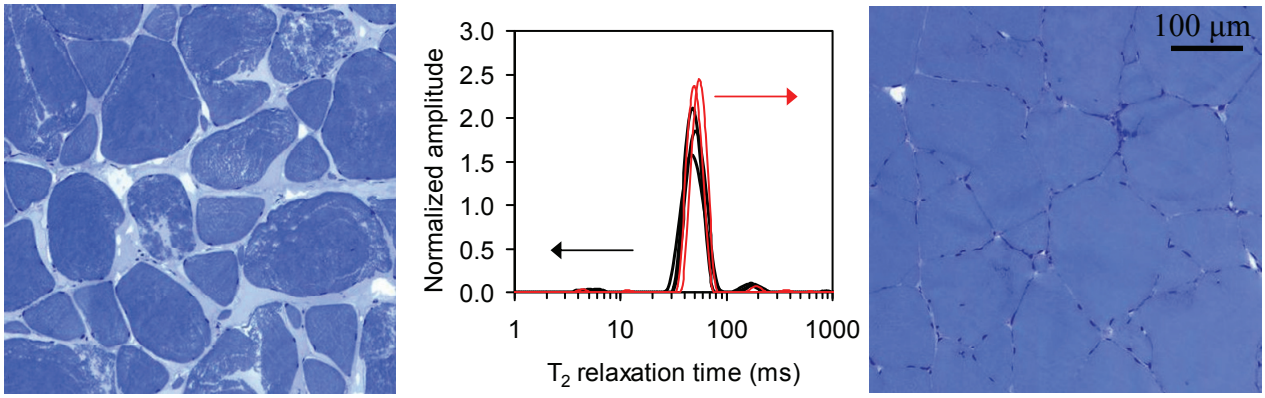

Figure 14: Light micrographs of salmon muscle tissue frozen/thawed (left) and frozen/thawed salted (right) and corresponding continuous distributed T_2 relaxation times of the same two samples.

In paper IV pronounced changes in T_2 relaxation characteristics were seen between pre- and post-rigor salmon. Lower relaxation times were observed for pre-rigor muscle indicating lower tissue water mobility. These observations were linked to striking differences in microstructure. The pre-rigor muscle displayed a dense architecture, and it was hard to discriminate the myofibers from each other, whereas the post-rigor muscle showed a less dense structure, and the myofibers were separated by a well-noticeable endomysium. T_2 relaxation proved to be a useful tool for investigation of post mortem events such as rigor mortis.

6.5 Raw material quality, ^{23}Na MRI and T_2 relaxation

As described in Chapter 3.4, factors like ionic strength and pH influence the microstructure and water binding of muscle (Offer and Knight, 1988; Offer and Trinick, 1983). This is especially reflected by salt-induced swelling of myofibers or by a change in pH. The amount of the muscle swelling depends on the salt concentration. At low salt concentrations above 0.1 M (physiological ionic strength) the muscle swells. Maximum swelling and maximum water holding capacity occur around 1 M (≈5.8% salt). Several authors have studied these changes by use of physico-chemical methods (Fennema, 1990; Offer and Trinick, 1983; Sigurgisladottir et al., 2000; Thorarinsdottir et al., 2002; 2004). Low-field NMR was applied to study salted pork meat (Wu et al., 2006; Andersen et al., 2007). However, the knowledge of T_2 relaxation dynamics during salting of meat is very limited at present, and even less research has been done on fish. A recent investigation showed that major changes in T_2 relaxation characteristics took place during salting of fatty (Atlantic salmon) and lean (Atlantic cod) fish in 15 and 25% NaCl (Paper V). An evident difference in water mobility shifts was observed between the two brine concentrations and species. **Figure 15** gives a summary of the changes in T_2 relaxation during salting.

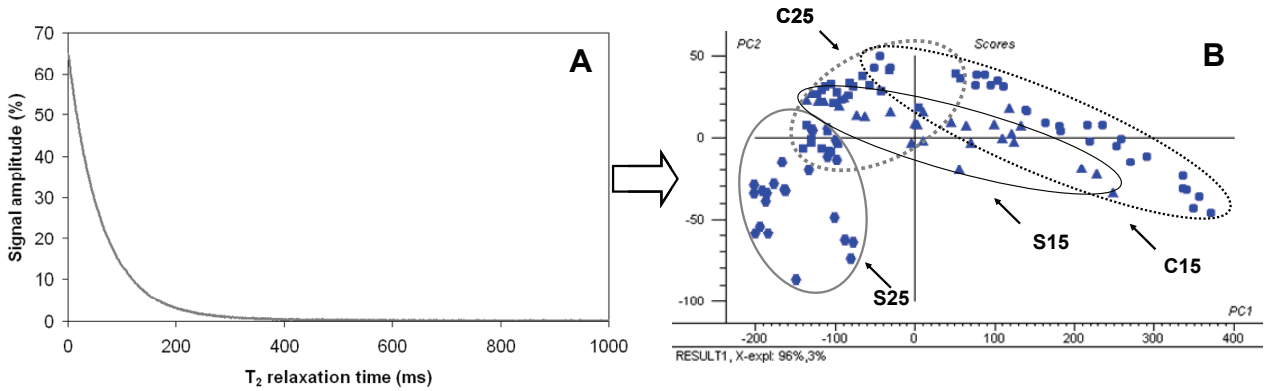

Figure 15: (a) Low-field NMR T_2 relaxation curve measured by CPMG pulse sequence; (b) PCA score plot of T_2 relaxation raw data obtained from salmon (S) and cod (C) fillets salted in 15 and 25% (w/w) brines (S15, C15, S25 and C25, respectively) for 14 days; samples were taken along the salting period (Aursand, M. et al., 2009, data from Paper V).

A clear tendency towards longer relaxation times was seen in 15% brine salted fillets, whereas a shift towards shorter relaxation times was seen in 25% brines. The most pronounced changes were seen in 15% brines, and changes tended to be faster in cod than in salmon. It was suggested that the "salting in" and "salting out" mechanisms for 15% brines and saturated brines, respectively, was reflected in the T_2 data. The knowledge of the biophysical effect of salting is limited at present, and this study must be considered as useful in the progress of obtaining a better understanding water dynamics and structural effects of salting. In the same study good linear correlations between physico-chemical analyses (WHC, centrifugation loss, water activity and salt content) and the T_2 relaxation data was obtained, and it was suggested that low-field NMR might be a useful supplement to the physico-chemical methods for analysis of product quality.

The progression of salt uptake is important because an even salt distribution is preferable as regards sensorial attributes, safety and water binding. A few ^{23}Na MRI studies have been performed on the salting of fish (Gallart-Jornet et al., 2007b, Foucat et al., 2006). Erikson et al. (2004) studied the salting and dehydration of Atlantic cod by use of ^{23}Na MR imaging and low-field NMR T_2 relaxation. However, the coupling of ^{1}H and ^{23}Na MRI with T_2 relaxation to study salting of fish is not common. In paper IV, pre-rigor, post-rigor and frozen/thawed fish constituted a model system in the investigation of water distribution and salt uptake and distribution affected by raw material quality. It was found that both post mortem status and freeze-thawing had a pronounced effect on salt distribution. These observations were coupled to differences in T_2 relaxation properties, hence, in general, shorter relaxation times and smaller T_{21} populations in unsalted raw material were linked to a lower salt uptake and sodium being more poorly distributed in the tissue. In Paper III

anaesthetized and exhausted fish were used as a model system to investigate the coupled effect of raw material quality on salt uptake and T_2 relaxation characteristics. An evident relationship between preslaugher conditions, salt uptake and tissue T_2 relaxation was obtained. As can be seen in **Figure 16,** clear differences in the T_{21} relaxation component was seen in the unsalted raw materials. Preslaugher stress clearly lead to a broader distribution of the T_{21} relaxation time constant and a shift towards longer relaxation times. These characteristics were coupled to a higher salt uptake and a more even distribution of NaCl within the muscle tissue. The results indicate that a combination of these two NMR techniques is a promising working method for obtaining further insight into the microstructure and water distribution of fish tissue and its effect on the salting process.

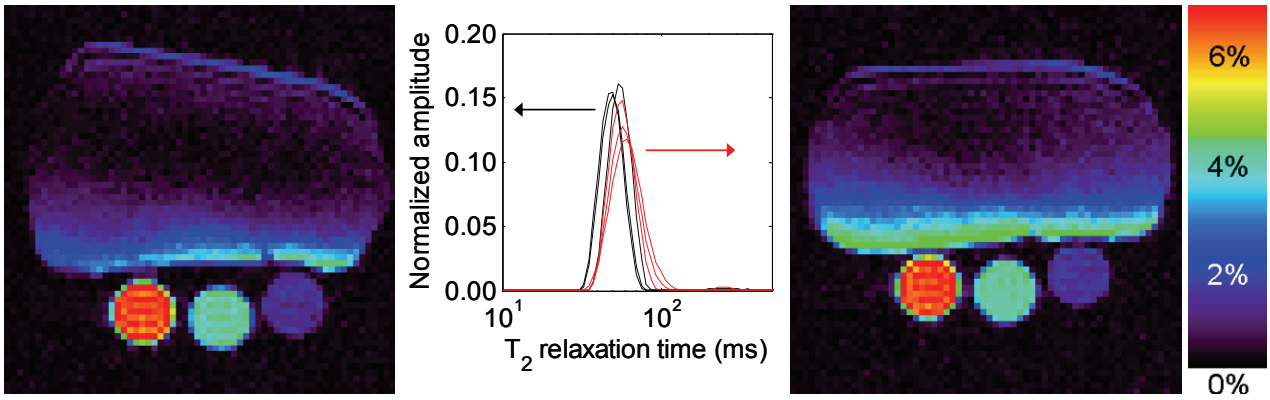

Figure 16: Distribution of T_2 relaxation times of white muscle tissue of anaesthetized (black curves) and exhausted (red curves) Atlantic salmon and the corresponding ^{23}Na MR images of the same fillets after brine salting, anaesthetized and exhausted to the left and right respectively (data from Paper III).

6.6 Freezing/thawing, heating and T_2 relaxation

Earlier T_2 relaxation studies on fish have been performed on lean cod muscle (Lambelet et al., 1995; Jensen et al 2002) and mince (Steen and Lambelet, 1997). Lambelet (1995) and Steen and Lambelet (1997) reported changes in water distribution during frozen-storage, whereas Jensen et al (2002) did not observe any changes due to freezing or chilled storage. In Paper II, a 2D diffusion weighted T_2 relaxation study was performed to compare the water distributions in fatty salmon muscle. A pronounced redistribution of water, reflected in the T_2 data as a decrease in T_{21} population, was seen as an effect of freezing/thawing. In paper IV, the same changes were observed, and they were linked to changes in the microstructure due to freeze-damage (Bello, 1982; Böcker, 2008).

Heating influences muscle foods with respect to its functional properties and its microstructure. A T_2 relaxation study of Atlantic salmon white and red muscle (Paper I) revealed pronounced changes

in water distribution at different temperatures from 4˚C to 55˚C. The changes in water mobility were suggested linked to structural alterations and denaturation of proteins as an effect of heating. Low-field NMR provided information about several features occurring as a result of heating. However, further studies needs to be done to fully understand the dynamics of water during heating of fish muscle.

6.7 Spatial fat and sodium distribution – ^{1}H and ^{23}Na MRI

Combined ^{1}H and ^{23}Na imaging of brine salted Atlantic salmon (Paper III and IV) revealed that the uptake and distribution of salt in the tissue was highly dependent on the spatial fat distribution. Subcutaneous fat acted as a barrier for the salt to diffuse into the tissue and salt uptake increases with decreasing fat content backwards the fillet. These findings are in agreement with earlier studies of brine salted Atlantic salmon (Foucat et al., 2006; Gallart-Jornet et al., 2007) and cod (Gallart-Jornet et al., 2007). Furthermore, MR imaging revealed that less sodium was distributed in the fatty areas located along the connective tissue (myocommata) (Paper III).

Today, one of the discussions concerning ^{23}Na MRI is the sodium visibility. In the work of this thesis a spin-echo based ^{23}Na MR imaging was applied. This technique is not fully quantitative, due to the partial MRI sodium invisibility (Springer, 1987; Bonny et al., 2001). However, the sodium MRI visibility is found to increase approximately linearly with water content in salmon and cod (Veliyulin and Aursand, 2009), and a negative correlation between the visibility and the protein content in minced meat was found (Veliyulin et al., 2009). Furthermore, the sodium visibility decreases with increasing tissue salt content (Veliyulin and Aursand, 2009; Veliyulin et al., 2009). In the studies of this thesis, MRI was applied on fillets with salt contents in the lower range (1-3 % NaCl). Furthermore, the technique was used for comparison of salt distribution between raw materials. It is therefore our opinion that the effect of sodium invisibility did not influence our conclusions.

7 Conclusions and future prospects

This thesis hopefully demonstrates that low-field NMR and MR imaging are methods of high potential as tools in the research of raw material quality, and fish processing. The techniques do not have a long history in the research of fish quality, and their applications are far from fully exploited. Despite that, low-field NMR and MR imaging has shown to give useful information about composition and raw material quality at different fish processing steps.

Regarding T_2 relaxation, this thesis has shown that the method can contribute to a further understanding of water dynamics in fish tissue. It is shown that T_2 relaxation components correlate well with traditional water analyses such as water holding capacity, centrifugation loss and water activity (Paper V). Furthermore, it has been established that the method is sensitive to fish species (Paper V), preslaughter stress (Paper III), rigor status (Paper IV), freezing/thawing (Paper II and IV), heating (Paper I) as well as brine salting with different NaCl concentrations and salting times (Paper III, IV and V). The tissue T_2 relaxation characteristics have been linked to microstructure, salt distribution and salt uptake. It has been suggested that entrapped and free water, and fat when present, give rise to the main relaxation components in fish muscle tissue. Further research needs to be conducted to understand the nature of the relaxation components. However, some day a full understanding of water interactions in muscle tissue may be obtained, and this will undoubtedly open many new doors in the research of water distribution and tissue structure.

Combined ^{1}H and ^{23}Na imaging of brine salted Atlantic salmon revealed that the uptake and distribution of salt in the tissue was highly dependent on the spatial fat distribution. Furthermore, an evident link was observed between T_2 relaxation characteristics and sodium distribution of salmon flesh. The combination of T_2 relaxaometry with MR imaging was proven to be a promising working method for obtaining further insight into the microstructure and water distribution of fish tissue and its effect on the salting process.

In this work, salting experiments were set up as simulation of industrial processes. By choosing this approach, results regarding i.e. salt uptake as a function of raw material quality can easier be transferred to the processing industry. However, it excludes the possibility to control the pH of the flesh during processing. Addition of salt is known to influence the muscle pH, and as earlier discussed, pH influences microstructure. To gain further knowledge on the link between microstructure and relaxation characteristics in fish tissue during salting, addition of buffers to adjust pH should be considered.

In the recent years, new ^{23}Na MRI techniques have been developed to overcome the problem of sodium invisibility. Using single-point ramped imaging with T_1 enhancement (SPRITE) MRI Romanzetti et al. (2006) were able to obtain ^{23}Na spin density maps of human brain. Later, the technique has been applied with success to salmon and cod (Veliyulin et al., 2007) as well as meat minces (Veliyulin et al., 2009). The technique makes it possible to study the bound fraction of sodium, and this issue should undoubtedly be considered for further work.

References

Alanen, A., Komu., M., Bodestam, S., Toikkanen, S. (1991) Determination of fat content of burbot (Lota lota) liver with low field MR imaging (0.04 T). *Physics in Medicine and Biology*, 36, 953-961.

Alberts, B., Bray, D., Johnsen, A., Lewis, J., Raff, M., Roberts, K., Walter, P. (1998) *Essential cell biology. An introduction to the molecular biology of the cell*. Garland publishing, Inc. New York. USA. (pp 538).

Andersen, R.H., Andersen, H.J., Bertram, H.C. (2007) Curing induced water mobility and distribution within intra- and extra myofibrillar spaces of three pork qualities. *International Journal of Food Science and Technology,* 42, 1059–1066.

Andersen, C.M., Jørgensen, B.M. (2004) On the relation between water pools and water holding capacity in cod muscle. *Journal of Aquatic Food Product Technology*, 13, 13–23.

Andersen, C.M., Rinnan, Å. (2002) Distribution of water in fresh cod. *Lebensmittel-Wissenshaft und Technologie.* 35, 687–696.

Aursand, M., Veliyulin, E., Standal, I.B., Falch, F., Aursand, I.G., Erikson, U. (2009) Process evaluation and quality assessment by NMR. In: Rehbein and Oehlenschläger (eds), Fishery products: Quality, Safety and Authenticity. Blackwell Publishing Limited, Oxford. In press.

Ayala, M.D., Albors, O.L, Blanco, A., Alcazar, A.G., Abellan, E., Zaroza, G.R. Gil, F. (2005) Structural and ultrastructural changes on muscle tissue of sea bass, *Dicentrarchus labrax* L., after cooking and freezing. *Aquaculture,* 250, 215-231.

Ballerini, L., Högberg, A., Borgefors, G., Bylund, A.-C., Lindgård. A., Lunström, K., Rakotonirainy, O., Soussi, B. (2002) A segmentation technique to determine fat content in NMR images of beef meat. *IEEE Transactions on Nuclear Science*, 49, 195-199.

Barat, J. M., Rodrıíguez-Barona, S., Andre´s, A., Fito, P. (2002) Influence of increasing brine concentration in the cod salting process. *Journal of Food Science.* 65, 1922–1925.

Barat, J. M., Rodríguez-Barona, S., Andres, A., Fito, P. (2003) Cod salting manufacturing analysis. *Food Research International.* 36, 447–453.

Bechmann, I.E., Pedersen, H.T., Nørgaard, L., Engelsen, S.B. (1998) Comparative chemometric analysis of transverse low-field 1H NMR relaxation data. Proceedings of the fourth international conference on applications of magnetic resonance in food science, Norwich, UK.

Bello, R.A.; Luft, J.H.; Pigott, G.M. (1981) Improved histological procedure for microscopic demonstration of related changes in fish muscle-tissue structure during holding and freezing. *Journal of Food Science,* 46, 733.

Bello, R.A., Luft, J.H., Piggot, G.M. (1982) Ultrastructural-study of skeletal fish muscle after freezing at different rates. *Journal of Food Science*, 47, 1389-1394.

Belton, P. (1990) Can nuclear magnetic resonance give useful information about the state of water on foodstuffs? *Comments Agricultural and Food Chemistry,* 2, 179-209.

Bendall, J.R., and Swatland, H.J. (1988) A review of the relationships of pH with physical aspects of pork quality. *Meat Science,* 24, 85–126.

Bertram, H.C., Andersen, H.J., Karlsson, A.H. (2001a) Comparative study of low-field NMR relaxation measurements and two traditional methods in the determination of water holding capacity of pork. *Meat Science*, 57, 125–132.

Bertram, H.C., Dønstrup, S., Karlsson, A.H., Andersen, H.J. (2002a) Continuous distribution analysis of T2 relaxation in meat – an approach in the determination of water-holding capacity. *Meat Science*, 60, 279–285.

Bertram, H.C., Karlsson, A.H., Rasmussen, M., Dønstrup, S., Petersen, O.D., Andersen, H.J. (2001b) The origin of multiexponential T2 relaxation in muscle myowater. *Journal of Agricultural and Food Chemistry*, 49, 3092–3100.

Bertram, H.C., Kristensen, M., Andersen, H.J. (2004) Functionality of myofibrillar proteins as affected by pH, ionic strength and heat treatment – a low-field NMR study. *Meat Science*, 68, 249–256.

Bertram, H.C., Purslow, P.P., Andersen, H.J. (2002b) Relationship between meat structure, water mobility, and distribution: a low-field nuclear magnetic resonance study. *Journal of Agricultural and Food Chemistry*, 50, 824–829.

Bloch, F., Hansen, W.W., Packard, M. (1946) Nuclear induction. *Physical Review*, 69, 127.

Blackband, S.J., Stoskopf, M.K. (1990) In vivo nuclear magnetic resonance imaging and spectroscopy of aquatic organisms. *Magnetic Resonance Imaging*, 8, 191–198.

Bock, C., Sartoris, F.-J., Pörtner, H.-O. (2002). In vivo MR spectroscopy and MR imaging on non-anaesthetized marine fish: techniques and first results. *Magnetic Resonance Imaging*, 20, 165–172.

Bonny, J.M., Laurent, W., Renou, J.P. (2001) Characterisation of meat structure by NMR imaging at high field, in *Magnetic Resonance in Food Science: A View to the Future*, ed. by Webb GA. Royal Society of Chemistry, Cambridge, UK, pp. 17–21.

Bremner, H.A. (1992) *Fish flesh structure and the role of collagen – its post-mortem aspects and implications for fish processing.* In H.H. Huss, M. Jacobsen & J. Liston (Eds.), Quality Assurance in the Fish Industry (pp 39-62). Amsterdam, The Netherlands: Elsevier Science Publishers B.V.

Bremner, H.A., Hallett, I.C. (1985) Muscle fiber-connective tissue junctions in the fish blue grenadier (*Macruronus novaezelandiae*). A scanning electron microscope study. *Journal of Food Science*, 50, 975-980.

Brown, R.J.S., Capozzi, F., Cavani, C., Cremonini, M.A., Petracci, M., Placucci, G. (2000) Relationships between 1H NMR relaxation data and some technological parameters of meat: A chemometric approach. *Journal of Magnetic Resonance*, 147, 89–94.

Brøndum, J., Munck, L., Henckel, P., Karlsson, A., Tornberg, E., Engelsen, S.B. (2000). Prediction of water-holding capacity and composition of porcine meat with comparative spectroscopy. *Meat Science*, 55, 177–185.

Carr, H.Y., Purcell, E.M. (1954) Effects of diffusion on free precession in nuclear magnetic resonance experiments. *American Journal of Physiology,* 94, 630–638.

Cole, W.C., Leblanc, A.D., Jhingran, S.G. (1993) The Origin of Biexponential T2 Relaxation in Muscle Water. *Magnetic Resonance in Medicine*, 29, 19-24.

Collewet, G., Toussaint, C., Davenel, A., Akoka, S., M´edale, F., Fauconneau, B., Haffray, P. (2001) *Magnetic resonance in food science: a view to the future.* In: GA Webb (Ed). Special Publication 262. Royal Soc. Chem., 0260–6291: Cambridge, p 252.

Diesbourg, L., Swatland, H.J., Millman, B.M. (1988) X-raydiffraction measurements of postmortem changes in the myofilament lattice of pork. *Journal of Animal Science*, 66, 1048–1054.

Duerr, J.D., Dyer, W.J. (1952) Proteins in fish muscle. Denaturation by salt. *Journal of the Fisheries Research Board*, 8, 325–331.

Dunajski, E. (1979) Texture of fish muscle. *Journal of Texture studies*, 10, 301-318.

Erikson, U. (2001) Rigor measurements. In: *Farmed Fish Quality* (S. Kestin and P. Wariss, Eds.), 283-297, Blackwell Science, Oxford, UK

Erikson, U., Misimi, E. (2008) Atlantic salmon skin and fillet color as affected by perimortem handling stress, rigor mortis and ice storage. *Journal of Food Science*, 73, C50-C59.

Erikson, U., Veliyulin, E., Singstad, T., Aursand, M. (2004) Salting and desalting of fresh and frozen-thawed cod (*Gadus morhua*) fillets: A comparative study using ^{23}Na NMR, ^{23}Na MRI, low-field ^{1}H NMR, and physicochemical analytical methods. *Journal of Food Science*, 69, 107–114.

Esaiassen, M., Østli, J., Joensen, S., Prytz, K., Olsen, J.V., Carlehög, M., Elvevoll, E.O., Richardsen, R. (2005) Brining of cod fillets: effects of phosphate, salt, glucose, ascorbate and starch on yield, sensory quality and consumers liking. *Food Science and Technology,* 38, 641–649.

Farrar, T.C. (1987) *An Introduction to Pulse NMR Spectroscopy*, The Farragut Press, Chicago, IL. pp 184.

Fennema, O.R. (1990) Comparative water holding properties of various muscle foods. A critical review relating to definitions, methods of measurement, governing factors, comparative data and mechanistic matters, *Journal of Muscle Foods,* 1, 363–381.

Fennema, O.R. (1985). *Water and ice*. In O. R. Fennema (Ed.), Food chemistry. New York: Marcel Dekker Inc.

Foegeding, E.A., Lanier, T.C. and Hultin, H.O. (1996) *Characteristics of edible muscle tissues*. In O.R. Fennema (Ed.), Food Chemistry. Third edition pp. 879-942. New York, USA: Marcel Dekker. Inc.

Foucat, L., Benderbous, S., Bielicki, G., Zanca, M., Renou, J.-P. (1995) Effect of brine injection on water dynamics in post-mortem muscle: Study of T2 and diffusion coefficients by MR microscopy. *Magnetic Resonance Imaging,* 13, 259-267.

Foucat, L., Taylor, R.G., Labas, R., Renou, J.P. (2001) Characterization of frozen fish by NMR imaging and histology. *American Laboratory*. 33, 38-43.

Foucat, L., Ofstad, R. Renou, J.P. (2006) How is the fish meat affected by technological processes? In *Modern Magnetic Resonance,* Webb, G. A., Ed.; Springer: The Netherlands, 957-961.

Gallart-Jornet, L., Rustad, T., Erikson, U., Barat, J. M., Escriche, I., Fito, P. (2007a) Influence of brine concentration on Atlantic salmon fillet salting. *Journal of Food Engineering.* 80, 267–275.

Gallart-Jornet, L., Barat, J.M., Rustad, T., Erikson, U., Escriche, I., Fito, P. (2007b) A comparative study of brine salting of Atlantic cod (*Gadus morhua*) and Atlantic salmon (*Salmo salar*). *Journal of Food Engineering*, 79, 261–270.

Guiheneuf, T.M., Duce, S.L., Gibbs, S.J., Hall, L.D. (1995) Use of magnetic resonance imaging to study the binding of manganese ions in brine-cured pork. *International Journal of Food Science Technology*, 30, 447-459.

Guiheneuf, T.M., Tessier, J.-J., Herrod, N.J., Hall, L.D. (1996) Magnetic resonance imaging of meat products: Automated quantitation of the NMR relaxation parameters of cured pork by both 'bulk' NMR and MRI methods. *Journal of the Science of Food and Agriculture*, 71, 163-173.

Guiheneuf, T.M., Parker, A.D., Tessier, J.J., Hall, L.D. (1997) Authetication of the effect of freezing/thawing of pork by quantitative magnetic resonance imaging. *Magnetic Resonance in Chemistry*, 35, 112-118.

Haard, N.F. (1992) Control of chemical composition and food wuality attributes of cultured fish. *Food Research International*, 25, 289-307.

Hall, L.D., Evans, S.D., Nott, K.P. (1998) Measurement of textural changes of food by MRI relaxometry. *Magnetic Resonance Imaging*, 16, 485-492.

Hamm, R. (1986) *Functional properties of the myofibrillar system and their measurements, in Muscle as Foods* (P.J. Bechtel, ed.) Academic press, New York, pp 130-200.

Hamm, R. (1960) Biochemistry of meat hydration. In *Advances in Food Research*, vol. 10. eds. C.O. Chichester and E.M. Mark, 355-463. New York London: Academic Press.

Hegarty, P.V. (1970). Differences in fibre size of histologically processed pre- and post-rigor mouse skeletal muscle. *Life Science,* 9, 443–449.

Hills, B. (1995) Food processing – an MRI perspective. *Trends in Food Science and Technology*, 6, 111–117.

Hills, B. (1998) *Magnetic Resonance Imaging in Food Science*. Wiley, New York, p. 96

Honikel, K.O., Kim, C.J., Hamm, R., Roncales, P. (1986) Sarcomere shortening of prerigor muscles and its influence on drip loss. *Meat Science,* 16, 267–282.

Honikel, K.O. (1989) The meat aspects of water and food quality. In *Water and Food Quality*, (ed. T.M. Hardman). London New York: Elsevier Applied Science.

Howell, N., Shavila, Y., Grootveld, M., Williams, S. (1996) Highresolution NMR and magnetic resonance imaging (MRI) studies on fresh and frozen cod (*Gadus morhua*) and haddock (*Melanogrammus aeglefinus*). *Journal of the Science of Food and Agriculture*, 72, 49–56.

Howgate, P. (1979) *Fish.* In: Food Microscopy*,* (ed. J.G. Vaughn), 343-392. London Academic Press.

Huff-Lonergan, E., Lonergan, S.M. (2005) Mechanisms of water-holding capacity of meat: The role of post-mortem biochemical and structural changes. *Meat Science,* 71, 194-204.

Jensen, K.N., Guldager, H.S., Jørgensen, B.M. (2002) Three-way modelling of NMR relaxation profiles from thawed cod muscle. *Journal of Aquatic Food Product Technology*, 11, 201–214.

Jensen, K.N., Jørgensen, B.M., Nielsen, H.H., Nielsen, J. (2005) Water distribution and mobility in herring muscle in relation to lipid content, season, fishing ground and biological parameters. *Journal of the Science of Food and Agriculture,* 85, 1259–1267.

Jepsen, S.M., Pedersen, H.T., Engelsen, S.B. (1999) Application of chemometrics to low-field 1H NMR relaxation data of intact fish flesh. *Journal of the Science of Food and Agriculture,* 79, 1793–1802.

Jittinandana, S., Kenney, P.B., Slider, S.D., Kiser, R.A. (2002) Effect of brine concentration and brining time on quality of smoked rainbow trout Fillet. *Journal of Food Science,* 67, 2095–2099.

Jolliffe, I.T. (1997) Principal Component Analysis; Springer-Verlag: Berlin, Germany.

Katikou, P., Hughes, S.I., Robb, D.H.F. (2001) Lipid distribution within Atlantic salmon (*Salmo salar*) fillets. *Aquaculture* 202:89-99.

Kerr, W.L., Reid, D.S., Kauten, R.J., McCarthy, M.J. (1998) Monitoring the formation of ice during food freezing by magnetic resonance imaging. *Lebensmittel-Wissenshaft & Technologie*, 31, 215-220.

Kiessling, A., Aasgaard, T., Storebakken, T., Johansson, L., Kiessling, K.-H. (1991) Changes in the structure and function of the epaxial muscle of rainbow trout *(Oncorhynchus mykiss)* in relation to ration and age. 111. Chemical composition. *Aquaculture* 93, 373-387.

Kiessling, A., Espe, M. Ruohonen, K., Mørkøre, T. (2004) Texture, gaping and colour of fresh and frozen Atlantic salmon flesh as affected by pre-slaughter iso-eugenol or CO_2 anaesthesia. *Aquaculture,* 236, 645-657.

Kivikari, R. (1996). Buffering capacity of meat. Thesis. University of Helsinki, EKT -series 1048.

Kristoffersen, S., Tobiassen, T., Esaiassen, M., Olsson, G.B., Godvik, A.L., Seppola, M.A., Olsen, R.L. (2006) Effects of pre-rigor on quality aspects of Atlantic cod (*Gadus morhua* L). *Aquaculture Research*, 37, 1556–1564.

Lambelet, P., Renevey, F., Kaabi, C., Raemy, A. (1995) Low-field nuclear magnetic resonance study of stored or processed cod. *Journal of Agricultural and Food Chemistry,* 43, 1462–1466.

Lauritzsen, K., Akse, L., Johansen, A., Joensen, S., Sørensen, N.K., Olsen, R.L. (2004) Physical and quality attributes of salted cod (*Gadus morhua,* L.) as affected by the state of rigor and freezing prior to salting. *Food Research International*, 37, 677–688.

Lauterbur, P.C. (1973) Image formation by induced local interactions: example employing nuclear magnetic resonance, *Nature*, 243:190.

Lillford, P.J., Clark, K.H., Jones, D.V. (1980) Distribution of water in heterogeneous foods and model systems. In *Water in Polymers*; Rowland, S.P., Ed.; American Chemical Society: Washington, DC, 177-195.

Løje, H., Green Petersen, D., Nielsen, J., Jørgensen, B.M., Jensen, K.N. (2007) Water distribution in smoked salmon. *Journal of the Science of Food and Agriculture,* 87, 212–217.

Martens, H., Martens, M. (2001) Multivariate analysis of quality: an introduction. Chichester, UK: John Wiley & Sons, Ltd.

Martínez-Álvarez, O., Gómez-Guillén, M.C. (2005) The effect of brine composition and pH on the yield and nature of water-soluble proteins extractable from brined muscle of cod (*Gadus morhua*). *Food Chemistry* 92, 71–77.

Meiboom, S., Gill, D. (1958) Modified spin-echo method for measuring nuclear times. *Review of Scientific Instruments,* 29, 688–691.

Micklander, E., Peshlov, B., Purslow, P.P., Engelsen, S.B. (2002) NMR cooking: monitoring the changes inmeat during cooking by lowfield 1H-NMR. *Trends in Food Science and Technology*, 13, 341–346.

Misimi, E. Erikson, U. Digre, H. Skavhaug, A. Mathiassen, J.R. (2008) Computer vision-based evaluation of preand postrigor changes in size and shape of Atlantic cod (Gadus morhua) and Atlantic salmon (Salmo salar) fillets during rigor mortis and ice storage: Effects of perimortem handling stress, *Journal of Food Science*, 73, E57-E68.

Mitchell, A.D., Wang, P.C., Rosebrough, R.W., Elasasser, T.H., Schmidt, W.F. (1991) Assessment of body composition of poultry by nuclear magnetic resonance imaging and spectroscopy. *Poultry Science*, 70, 2494-2500.

Mulkern, R.V. Spencer, R.G.S. (1988) Diffusion imaging with paired CPMG sequences. *Magnetic Resonance in Medicine,* 6: 623–631.

Murray, J., Burt, J.R. (1969). The composition of fish. *Torry Advisory Notes* 38, Torry Research Station, Aberdeen.

Nakayama, T., Da-Jia, L., Ooi, A. (1992) Tension changes of stressed and unstressed carp muscle isometric rigor contraction and resolution. *Nippon Suisan Gakkaishi*, 58, 1517–1522.

Ngapo, T.M., Babare, I.H., Reynolds, J., Mawson, R.F. (1999) Freezing rage and frozen storage effects on the ultrastructure of samples of pork. *Meat Science*, 53, 159-168.

Nott, K.P., Evans, S.D., Hall, L.D. (1999a) The effect of freeze-thawing on the magnetic. Resonance imaging parameters of cod and mackerel. *Lebensmittel-Wissenshaft and Technologie* 32, 261.

Nott, K.P., Evans, S.D., Hall, L.D. (1999b) Quantitative magnetic resonance imaging of fresh and frozen-thawed trout. *Magnetic Resonance Imaging* 17, 445–455.

Næs, T., Isakssson, T., Fearn, T., Davies, D. (2002) A user-friendly guide to multivariate calibration and classification. Chichester, UK: NIR Publications.

NFSA, Norwegian Food Safety Authority (2008) The Norwegian Food Composition Table 2009. www.matportalen.no/matvaretabellen, 05.05 2009.

Nielsen, D., Hyldig, G., Nielsen, J., Nielsen, H.H. (2005) Lipid content in herring (Clupea harengus L) influence of biological factors and comparison of different methods of analyses: Solvent extraction, Fatmeter, NIR and NMR. *Food Science Technology*, 38, 537-548.

NIFES, Norwegian Institute of Nutrition and Seafood Research (2008) Seafood data. www.nifes.no, 05.05 2009.

Offer, G. (1991) Modeling of the formation of pale, soft and exudative meat – effects of chilling regime and rate and extent of glycolysis. *Meat Science,* 30, 157–184.

Offer, G., Cousins, T. (1992) The mechanism of drip production – formation of 2 compartments of extracellular-space in muscle postmortem. *Journal of the Science of Food and Agriculture*, 58, 107–116.

Offer, G., Knight, P. (1988a) The structural basis of water-holding capacity in meat. Part 1: general principles and water uptake in meat processing. In R. Lawrie (Ed.). *Developments in meat science*, New York: Elsevier Applied Science vol. 4, 61–171.

Offer, G., Knight, P. (1988b) The structural basis of water-holding capacity in meat. Part 2: drip losses. In R. Lawrie (Ed.). Developments in meat science, London: Elsevier Science Publications, vol. 4, 173–243.

Offer, G., Knight, P., Jeacocke, R., Almond, R., Cousins, T., Elsey, J., (1989) The structural basis of the water-holding, appearance and toughness of meat and meat-products. *Food Microstructure,* 8, 151–170.

Offer, G., Trinick, J. (1983) On the mechanism of water holding in meat: the swelling and shrinking of myofibrils. *Meat Science*, 8, 245–281.

Pedersen, H.T., Berg, H., Lundby, F. Engelsen, S.B. (2001) The multivariate adcantage in fat determiantion in meat by bench-top NMR. *Innovative Food Science and Emerging Technologies*, 2, 87-94.

Provencher, S. W. (1982) A constrained regularization method for inverting data represented by liner algebraic of integral equations. *Computer Physics Communications,* 27, 213–227.

Purcell, E.M., Torrey, H.C., Pound, R.V. (1946) Resonance absorption by nuclear magnetic moments in a solid. *Physical Review,* 69, 37-38.

Puolanne, E.J., Ruusunen, M.H., Vainionpää J.I. (2001) Combined effects of NaCl and raw meat pH on water-holding in cooked sausage with and without added phosphate, *Meat Science*, 58, 1-7.

Renou, J.P., Monin, G., Sellier, P. (1985a) Nuclear magnetic resonance measurements on pork of various qualities. *Meat Science*, 15, 225–233.

Renou, J.P., Benderbous, S., Bielicki, B., Foucat, L., Donnat, J.P. (1994) ^{23}Na magnetic resonance imaging: distribution of brine in muscle. *Magnetic Resonance Imaging,* 12, 131–137.

Renou, J.P., Kopp, J., Valin, C. (1985b) Use of low resolution NMR for determining fat content in meat products, *Journal of Food Technology*, 20, 23-29.

Robb, D.H.F., Kestin, S.C., Warriss, P.D., (2000) Muscle activity at slaughter: I. Changes in flesh colour and gaping in rainbow trout. *Aquaculture* 182, 261–269.

Romanzetti, S., Halse, M., Kaffanke, J., Zilles, K., Balcom, B.J., Shah, N.J. (2006) A comparison of three SPRITE techniques for the quantitative 3D imaging of the 23Na spin density on a 4T whole-body machine. *Journal of Magnetic Resonance,* 179, 56–64.

Ruan, R.R., Chen P.L. (2001) Nuclear magnetic resonance techniques and their application in food quality analysis, in *Nondestructive Food Evaluation;* Gunasekaran, S. Ed.; Marcel Dekker Inc.: New York, 165-216.

Rørå, A.M.; Furuhaug, R.; Fjaera, S.O.; Skjervold, P.O. (2004) Salt diffusion in pre-rigor filleted Atlantic salmon. *Aquaculture*, 232, 201–211.

Rørå, A. M.; Kvale, A.; Mørkøre, T.; Rørvik, K. A.; Steien, S. H.; Thomassen, M. S. (1999) Process yield, colour and sensory quality of smoked Atlantic salmon (Salmo salar) in relation to raw material characteristics. *Food Research International,* 31, 601–609.

Sannaveerappa, T., Ammu, K., Joseph, J. (2004) Protein-related changes during salting of milkfish (*Chanos chanos*). *Journal of the. Science of Food and Agriculture* 84, 863–869.

Scholz, A., Mitchell, A.D., Wang, P.C., Song, H., Yan, Z. (1995) Muscle metabolism and body compostion of pigs with different ryanodine receptor genotypes studied by means of 31P nuclear magnetic resonance spectroscopy and 1H magnetic resonance imaging. *Archiv Tierzucht*, 38, 539-552.

Skjervold, P.O., Fjaera, S.O., Østby, P.B., Isaksson, T., Einen, O., Talyor, R. (2001a) Properties of salmon flesh from different locations on pre- and post-rigor fillets. *Aquaculture,* 201, 91–106.

Skjervold, P.O., Rørå, A.M.B., Fjaera, S.O., Vegusdal, A., Vorre, A., Einen, O. (2001b) Effects of pre-, in-, or post-rigor filleting of live chilled Atlantic salmon. *Aquaculture,* 194, 315–326.

Sigurgisladottir, S., Ingvarsdottir, H., Torrissen, O. J., Cardinal, M., Hafsteinsson, H. (2000) Effects of freezing/thawing on the microstructure and the texture of smoked Atlantic salmon (Salmo salar). *Food Research International,* 33, 857–865.

Stien, L.H., Hirmas, E., Bjørnevik, M., Karlsen, Ø., Nortvedt, R., Rørå, A.M.B., Sunde, J., Kiessling, A. (2005) The effects of stress and storage temperature on the color and texture of pre-rigor filleted cod (*Gadus morhua* L.). *Aquaculture Research*, 36, 1197-1206.

Springer C.S., Measurement of metal cation compartmentalization in tissue by high-resolution metal cation NMR. *Annual Review of Biophysics and Biophysical Chemistry* **16**:375–399 (1987).

Steen, C., Lambelet, P. (1997) Texture changes in frozen cod mince measured by low-field nuclear magnetic resonance spectroscopy. *Journal of the Science of Food and Agriculture,* 75, 268–272.

Sun, D.W., Zheng, C. (2007) *Computer vision technology for food quality evaluation.* Ed.: Sun D.W., Food science and technology: International series. Elsevier. Academic press. pp. 583.

Sørensen, N.K., Brataas, R., Nyvold, T.E., Lauritzen, K. (1997) Influence of early processing (pre-rigor) on fish quality. In: Luten JB, Børresen T, Oehlenschlaeger J, editors. Seafoods from producer to consumer, integrated approach to quality. Amsterdam: Elsevier. p 253-263.

Swatland, H.J., Belfry, S. (1985) Post-mortem changes in the shape and size of myofibrils from skeletal-muscle of pigs. *Mikroskopie*, 42, 26–34.

Thorarinsdottir, K.A., Arason, S., Bogason, S., Kristbergsson, K. (2004) The effects of various salt concentrations during brine curing of cod. *International Journal of Food Science and Technology,* 39, 79–89.

Thorarinsdottir, K.A., Arason, S., Geirsdottir, M., Bogason, S., Kristbergsson, K. (2002) Changes in myofibrillar proteins during processing of salted cod (*Gadus morhua*) as determined by electrophoresis and differential scanning calorimetry. *Food Chemistry,* 77, 377–385.

Thybo, A.K., Bechmann, I.E., Martens, M., Engelsen, S.B. (2000) Prediction of sensory texture of cooked potatoes using uniaxial compression, near infrared spectroscopy and low field H-1 NMR spectroscopy. *Food Science and Technology, Lebensmittel-Wissenshaft und Technologie*, 33, 103-111

Thygesen, L.G., Thybo, A.K., Engelsen, S.B. (2001) Prediction of sensory texture quality of boiled potatoes from low field ^{1}H NMR of raw potatoes. The role of chemical constituents. *Food Science and Technology, Lebensmittel-Wissenshaft andTechnologie,* 34, 469-477

Tingle, J.M., Pope, J.M., Baumgartner, P.A., Sarafis, V. (1995) Magnetic Resonance Imaging of fat and muscle distribution in meat. *International Journal of Food Science and Technology,* 30, 437–446.

Tornberg, E., Andersson, A., Aransson, G, von Seth, G. (1993) Water and fat distribution in pork in relation to sensory properties. In: Pork Quality: Genetic and Metabolic Factors (edited byE. Puolanne D.I. Demeyer M. Ruusunen & S. Ellis). Wallingford: CAB International.

Tornberg, E., Wahlgren, N.M., Brøndum, J., Engelsen, S.B. (2000). Pre-rigor conditions in beef under varying temperature- and pH-falls studied with rigometer, NMR and NIR. *Food Chemistry*, 69, 407–418.

Tornberg, E. (2005). Effects of heat on meat proteins – Implications on structure and quality on meat products. *Meat Science*, 70, 493-508.

Toussaint, C., Fauconneau, B., Médale, F., Collewet, G., Akoka, S., Haffray, P. Davenel, A. (2005) Description of the heterogeneity of lipid distribution in the flesh of brown trout (*Salmo trutta*) by MR imaging. *Aquaculture,* 243, 255–267.

Toussaint, C.A., Médale, F., Davenel, A., Fauconneau, B., Haffray, P., Akoka, S. (2001) Determination of the lipid content in fish muscle by a self-calibrated NMR relaxometry method: comparison with classical chemical extraction methods. *Journal of the Science of Food Agriculture,* 82, 173–178.

Tsoref, L., Shinar, H., Seo, Y., Eliav, U., Navon, G. (1998) Proton double quantum filtered MRI – a new method for imaging ordered tissues. *Magnetic Resonance in Medicine,* 40, 720–726.

Venugopal, V., Shahidi, F. (1996) Structure and composition of fish muscle. *Food Reviews International,* 12, 175-197.

Veliyulin, E., van der Zwaag, C., Burk, W., Erikson, U. (2005) In-vivo determination of fat content in Atlantic salmon (Salmo salar) with a mobile NMR spectrometer, *Journal of Science of Food and Agriculture*, 85, 1299-1304.

Veliyulin, E., Borge, A., Singstad, T., Gribbestad, I. and Erikson, U. (2006a) Post-mortem studies of fish using magnetic resonance imaging, *In*: *Modern Magnetic Resonance* (G. A. Webb, Ed.) Springer, The Netherlands, 949-956.

Veliyulin, E., Østerhus, K., Burk, W., Singstad, T. and Skjetne, T. (2006b) Comprehensive compositionalanalysis of fish feed by time domain NMR. In: G.A. Webb (Ed.) *Modern Magn. Reson*., Springer, The Netherlands, 887–893.

Veliyulin, E. and Aursand, I.G. (2007) 1H and 23Na MRI studies of Atlantic salmon (Salmo salar) and Atlantic cod (Gadus morhua) fillet pieces salted in different brine concentrations, *Journal of the Science of Food and Agriculture*, 87, 2676–2683.

Veliyulin, E., Egelandsdal, B., Marica, F., Balcom, B.J. (2009) Quantitative ^{23}Na Magnetic Resonance Imaging of Model Foods; *Journal of Agricultural and Food Chemistry*, In press.

Watt, B.K., Merrill, A.L. (1963) Composition of foods. Agriculture Handbook No. 8, Washington DC: US Department of Agriculture.

Wang, D., Correia, L.R., Tang, L. (1998) Modeling of salt diffusion in Atlantic salmon muscle. *Canadian Agricultural Engineering,* 40, 29–34.

Wang, D., Tang, J., Correia, L.R. (2000) Salt diffusivities and salt diffusion in farmed Atlantic salmon muscle as influenced by rigor mortis. *Journal of Food Engineering,* 43, 115–123.

Wright, D.J., Wilding, P. (1984) Differential scanning calorimetric study of muscle and its proteins: myosin and its subfragments. *J. Sci. Food Agric.*, 35, 357-372.

Wu, Z., Bertram, H.C., Kohler, A., Böcker, U., Ofstad, R., Andersen, H.J. (2006) Influence of aging and salting on protein secondary structures and water distribution in uncooked and cooked pork. A combined FT-IR microspectroscopy and 1H NMR relaxometry study. *J. Agric. Food Chem.,* 54, 8589–8597.

Yano, S., Tanaka, M, Suzuki, N, Kanzaki, Y (2002) Texture changes of been and salmon meats caused by refrigeration and use of pulse NMR as an index of taste. *Food Science and Technology Research*, 8, 137-143.

PART 2

Paper I

)ó Î Ïô ÉÎÃÌÕÄÅÄ ÄÕÅ ôÏ Ã ÏÐÙÒÉÇÈÔ

Paper II

STUDY OF FAT AND WATER IN ATLANTIC SALMON MUSCLE (*SALMO SALAR*) BY LOW FIELD NMR AND MRI

E. Veliyulin, I. G. Aursand and U. Erikson

SINTEF Fisheries and Aquaculture, 7465 Trondheim, Norway

1 INTRODUCTION

Development of non-destructive methods for studying the interactions of water and fat with the structure changes occurring during fish processing may provide the insight necessary to improve the quality of such products.

Various modalities of Nuclear Magnetic Resonance (NMR) offer several non-destructive applications that can provide with versatile information about the structure of various biological systems. Low field (LF) NMR has mainly been used for relaxation time studies and quantification of various components such as water and fat in foods. The microscopic structure of biological systems consists of a network of macromolecules that interact with water protons. Also, water is physically localized in various compartments in the tissues. ^{1}H NMR relaxation spectra of such systems may be complicated as the NMR responses from different ^{1}H pools are usually observed simultaneously and it is not always possible to separate relaxation contributions originating from different pools or different substances (for example fat and water). Interpretation of the NMR relaxation spectra is still a matter of discussion due to the complexity biological systems. For instance, in pork the simple intra-/extracellular compartmentalization theory suggested earlier[1] could not satisfactory explain all features of the multiexponential transverse relaxation. Three commonly observed relaxation components are attributed to the water tightly associated with macromolecules (the fastest relaxation component at 1–10 ms), water located within highly organized protein structures (the intermediate component at 40-60 ms), and water between fiber bundles (the slowest component at 150-400 ms)[2]. In fatty fish such as Atlantic salmon, the interpretation of relaxation spectra is complicated by the fact that the fat relaxation components interfere with those of water[3].

Magnetic Resonance Imaging (MRI) is a technique that offers a unique opportunity to produce cross-section images of intact whole fish. Depending on the particular task, MRI instruments can produce different types of visible contrast in the MR images. This is achieved by programming and running specific MR sequences that can differentiate the NMR response of the protons localized in molecules with different mobility or chemical environment. For example, it is possible to obtain MR images of 'water' and 'fat'[4], 'diffusion weighted' images where only molecules with low mobility are visible[5] or high resolution images of connective tissue[6]. A newly developed method based on double-quantum filtered MRI detects only molecules associated with ordered tissue structures,

suppressing the signal from isotropic fluids[7]. MRI is also a powerful technique to visualize and monitor various dynamic processes, allowing to dynamically follow processes non-destructively and with high spatial resolution. For instance combined with NMR spectroscopy MRI can be a valuable tool for studies of fresh and frozen fish[8].

The goal of the present study was to separate fat and water in fatty fish by: (1) showing the advantages of the 2D diffusion weighted T_2 relaxation method compared with the conventional 1D relaxation method, and (2) to develop MRI protocols to produce separate, quantitative 'fat' and 'water' images.

2 EXPERIMENTAL

2.1 LF NMR: Diffusion weighted transversal relaxation time studies

A farmed Atlantic salmon (*Salmo salar*) fillet was bought at the local fish market three days post mortem. Three parallel samples of the white muscle close to the belly flap area were stamped out of the fillet using a specially designed coring tool. Then the samples were transferred to NMR tubes (10 mm in diameter). The tube filling height was about 1 cm and the approximate sample weight was 0.4 g. After the LF NMR measurements, the NMR tubes containing samples were frozen at –25 °C (24 h) and thawed at 5 °C before repeating the measurements at 10 and 25 °C.

The LF measurements were performed using the minispec mq NMR analyzer (Bruker Optik GmbH, Germany) with a magnetic field strength of 0.47 Tesla corresponding to a proton resonance frequency of 20 MHz. The instrument is equipped with gradient coils producing magnetic field gradients of up to 3.2 Tesla/m. A water bath (Haake UWK 45, Germany) was connected to the probehead to make measurements at 10 or 25 ^{o}C regulating the sample temperature with an accuracy of 0.1°C. Before measurements, all samples were thermostated to 10 or 25 ^{o}C for 1 hour in a separate water bath (Julabo F10, Germany).

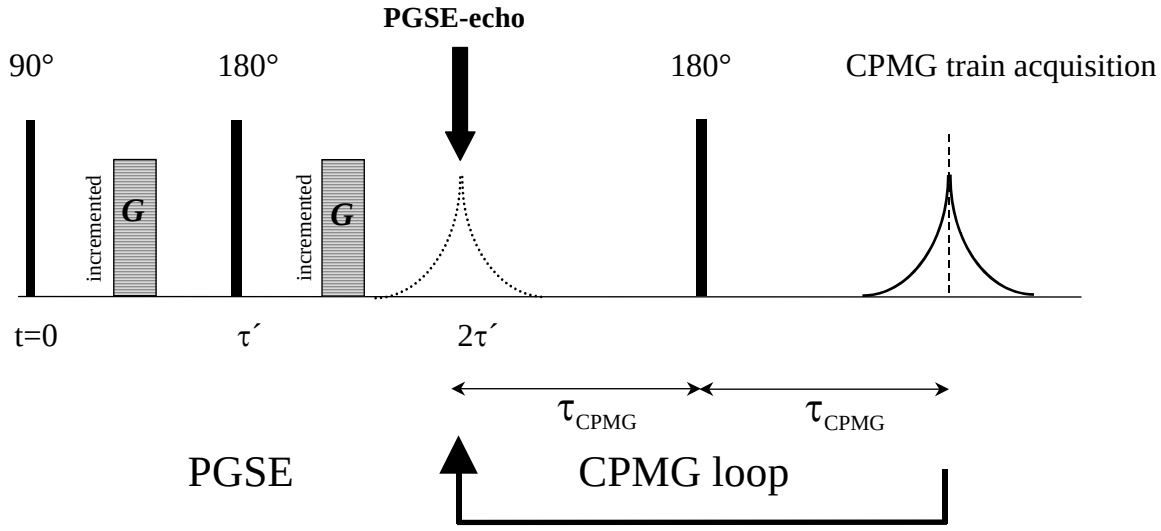

Figure 1 *The PGSE-CPMG pulse sequence for 2D diffusion vs. transversal relaxation time studies*

To obtain a two-dimensional data set of diffusion weighted transversal relaxation curves, a modification of the well-known Carr-Purcell-Meiboom-Gill (CPMG) pulse sequence was used. A pulsed field gradient spin echo sequence (PGSE) was combined with a train of 180° refocusing pulses (Figure 1). The amplitude of the PGSE gradients was incremented in steps (0.16 Tesla/m) from 0 to about 3.2 Tesla/m, increasingly suppressing the contribution of the most mobile components to the resulting echo. Corresponding relaxation curves were acquired at each gradient step. The following acquisition parameters were used: echo-time (TE) of the PGSE part of the sequence was set to 20 ms, duration of the gradient pulses was 1 ms, TE of the CPMG train was 0.2 ms, relaxation delay (RD) was 2 s and 4000 even echoes were acquired in 8 scans. Thus, a 2D data set with 4000 rows (dimension of relaxation) and 21 columns (dimension of diffusion) was obtained for each sample. In addition, conventional CPMG relaxation curves were measured for all samples with the same acquisition parameters as the CPMG echo train in the 2D experiment.

The 2D data were processed by the newly developed 2-D Inverse Laplace Transform[9], using software package[10] implemented in MatLab (The MathWorks, Inc., USA). The same software was used for processing of the 1D relaxation curves.

2.2 MRI: Quantification of white muscle fat and water

The MRI studies were performed using a Bruker Avance DBX100 instrument (Bruker BioSpin, Germany). The instrument has a horizontal wide bore opening suitable for imaging of comparatively large objects (^{1}H imaging area - sizes up to 15 cm in diameter and 15 cm in length).

The chemical shift selective (CHESS) imaging protocol makes use of the fact that the protons in fat and water molecules have slightly different NMR resonance frequency. Hence they have different chemical shifts. When using the technique, a special frequency selective RF pulse with a predefined bandwidth is applied to excite either the fat or the water component only. This makes it possible to achieve an acceptable degree of separation. Thus, separation of fat and water in MR images can be achieved.

A piece of frozen-thawed Atlantic salmon white muscle (approximately $3 \times 3 \times 4$ cm) was placed in the iso-center of the magnet. In addition, two reference samples containing 100 % fish oil and 100% distilled water were placed within the imaged area. The water reference was doped with 0.0001 m/l $MnCl_2$ to shorten the proton relaxation time to T_2 = 260 ms. Three types of MRI images were acquired: 'a proton density' image, 'a fat image' and 'a water image'. The following acquisition parameters were used: RD = 2 s, number of excitations (NEX) = 40, field of view (FOV) = 5 x 5 cm and TE = 16.2 ms (fat images) and 26.4 ms (water images). Images of 20 slices with a slice thickness of 1.5 mm were acquired. For fat excitation, a selective sinc-shaped pulse with a bandwidth (BW) of 700Hz was centered (CF) -600 Hz away from the water frequency to avoid signal contribution from water. For water signal excitation, a similar sinc pulse with a bandwidth of 480 Hz was centered +200Hz away from the water resonance frequency to avoid signal contribution from the fat (Figure 2). The ‘proton density’ image was acquired using a Multi-Spin Multi-Echo (MSME) protocol with TE = 4.1 ms, TR = 2 s and NEX = 4.

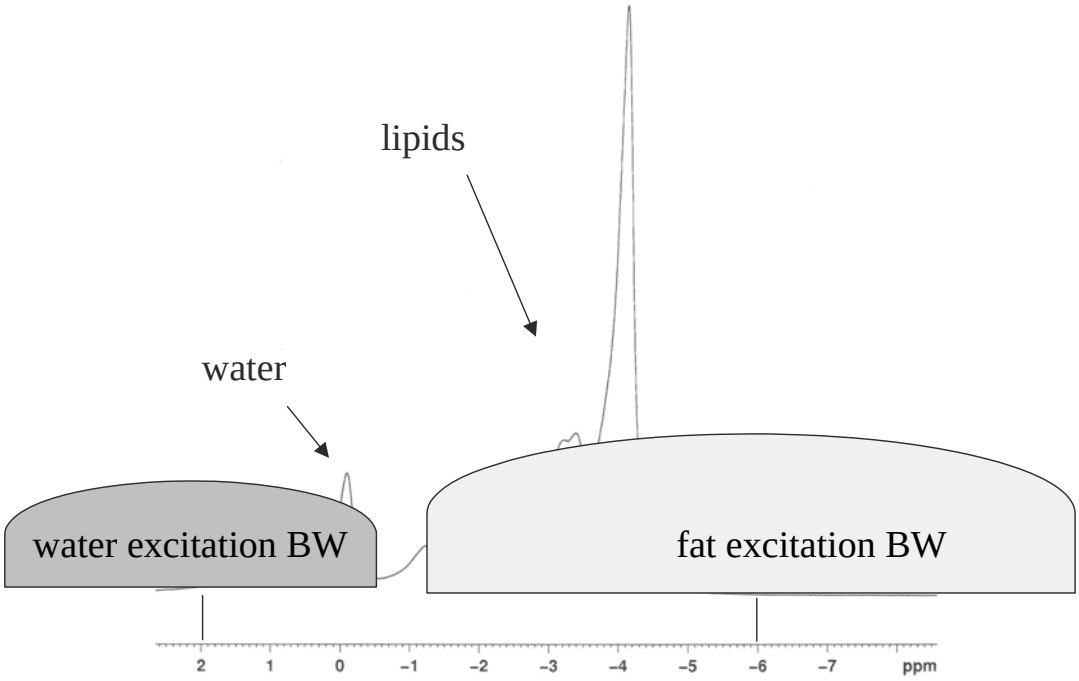

Figure 2 *Selective water (CF = +200 Hz, BW =480 Hz) and fat (CF = -600 Hz, BW = 700 Hz) excitation in the CHESS MRI protocols*

The obtained 'fat' and 'water' images were quantified with an in-house made MRI software package using the Interactive Data Language (Research Systems Inc., UK). Prior to calculation, the original images were scaled in the intensity range from 0 to 255. A histogram of all pixel intensities from the 'water' image is shown in Figure 3a. In this histogram the first peak (approximate intensity range 0 – 43) represents the noise in the image, the second peak (intensity range 43 – 150) originates from the salmon sample and the third one (intensity range 150 – 255) originates from the water reference. In order to quantify the water content, the 'noise' peak was first filtered out using the minimum between the 'noise' and the 'water' peaks (see Figure 3a) as a cut-off value. After that, the average intensity of the reference oil sample was set to 100 and the rest of the image pixel intensities were rescaled accordingly, resulting in a histogram as shown in Figure 3b. When calculating the mean intensity for all sample pixels of the modified image, the water content in the corresponding MRI slice could be determined. By averaging the water content of all slices (covering practically the whole sample), the mean water content of the whole sample was determined. Since the T_2 relaxation time of the sample (≈ 44 ms) was different from that of the water reference (260 ms), the calculated intensities had to be corrected correspondingly. An identical algorithm was used to determine the sample fat content. The programmed automated calculation routines could calculate fat and water contents in all image slices in about 20 s. After the MRI experiment, the salmon sample was divided in two equal parts, one for fat content determination by chemical extraction[11], while the other part was used for total water content determination by weight change after drying at 105 °C for 24 h.

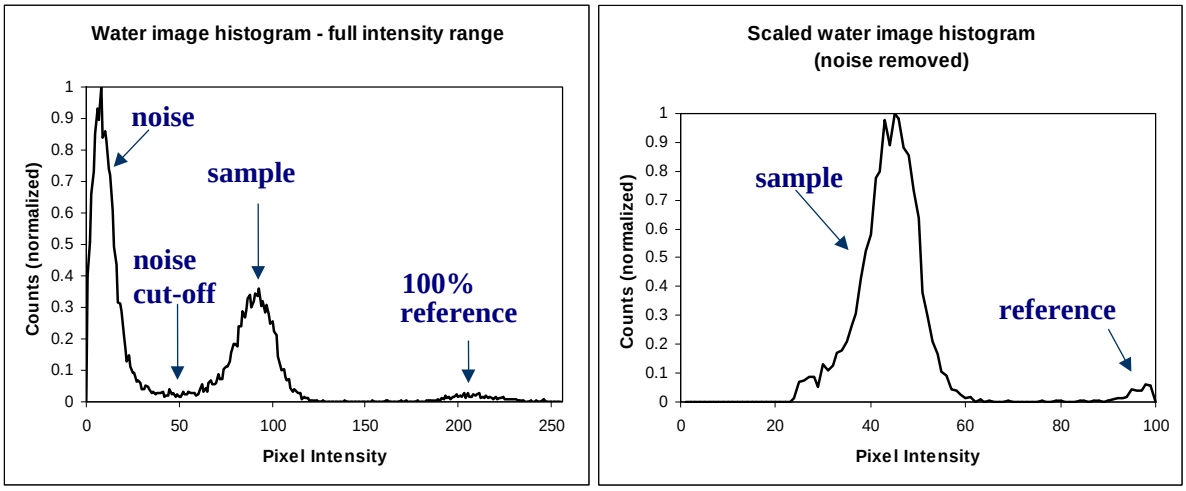

a) b)

Figure 3 *a) Pixel intensity histogram as acquired from the original 'water' image; b) Same histogram after noise filtering and rescaling*

3 RESULTS AND DISCUSSION

3.1 Diffusion weighted transversal relaxation time studies

Figure 4 shows diffusion vs. T_2 relaxation time distribution maps for fresh (10°C) and frozen-thawed muscle at 10 or 25 °C, respectively. The corresponding 1D T_2 distributions are the shown above the maps. From the 2D distribution maps the relaxation times and corresponding diffusion constants for the observed peaks could be roughly estimated. A water peak ($T_2 \approx 44$ ms, $D \approx 1.0\times10^{-9}$ m^2/s) and a fat peak ($T_2 \approx 100$ ms, $D \approx 2.7\times10^{-11}$ m^2/s) were observed in the fresh sample at 10°C. No clear changes was observed between fresh and frozen-thawed tissues when measured at 10°C. An advantage of the 2D distribution map approach compared with the conventional 1D is seen by inspecting the longer relaxation peak ($T_2 \approx 140$ ms) from the frozen-thawed sample measured at 25 °C. While the respective water and fat peaks completely overlap on the 1D distribution, the 2D map clearly shows the presence of the two phases at this relaxation time. At relaxation times about 140 ms, the diffusion constants at 25°C were 2.0×10^{-9} (water) and 2.6×10^{-10} m^2/s (fat), respectively. The water component with the longer relaxation time corresponds to that observed in cod[12,13] and pork muscle[2,14], which is thought to represent extra-myofibrillar water. After increasing the temperature from 10 to 25 °C a shift towards slightly shorter relaxation time and higher diffusion constant was observed for the major water component ($T_2 \approx 37$ ms, $D \approx 2.0\times10^{-9}$ m^2/s). In a marine coldwater species such as Atlantic salmon, the tissues contain polyunsaturated fatty acids. This fraction of the total fat content is mobile even at very low temperatures. Therefore, more research is needed to elucidate the "NMR-behavior" of this fat as seen in relation to changes in the extramyofibrillar water pool.

The technique may be improved in order to further minimize the effect of Eddy-currents on the observed CPMG echo train. This would allow running the PGSE pulse sequence at substantially shorter echo times making it possible to obtain information about

the fast relaxing components such as water bound to macromolecules and immobile fat. Further development of the data processing software would allow separate quantification of various water pools and lipids by 2D integration of the corresponding peaks. The method can be valuable for investigation of several types of complex food systems, detecting the presence of different water and fat phases in the sample. Furthermore, 2D diffusion weighted relaxation experiments performed under different food processing conditions (temperature, pressure, humidity, salt content etc.) may be useful to provide a better understanding of the system. In turn, this information can be used to optimize various food unit operations.

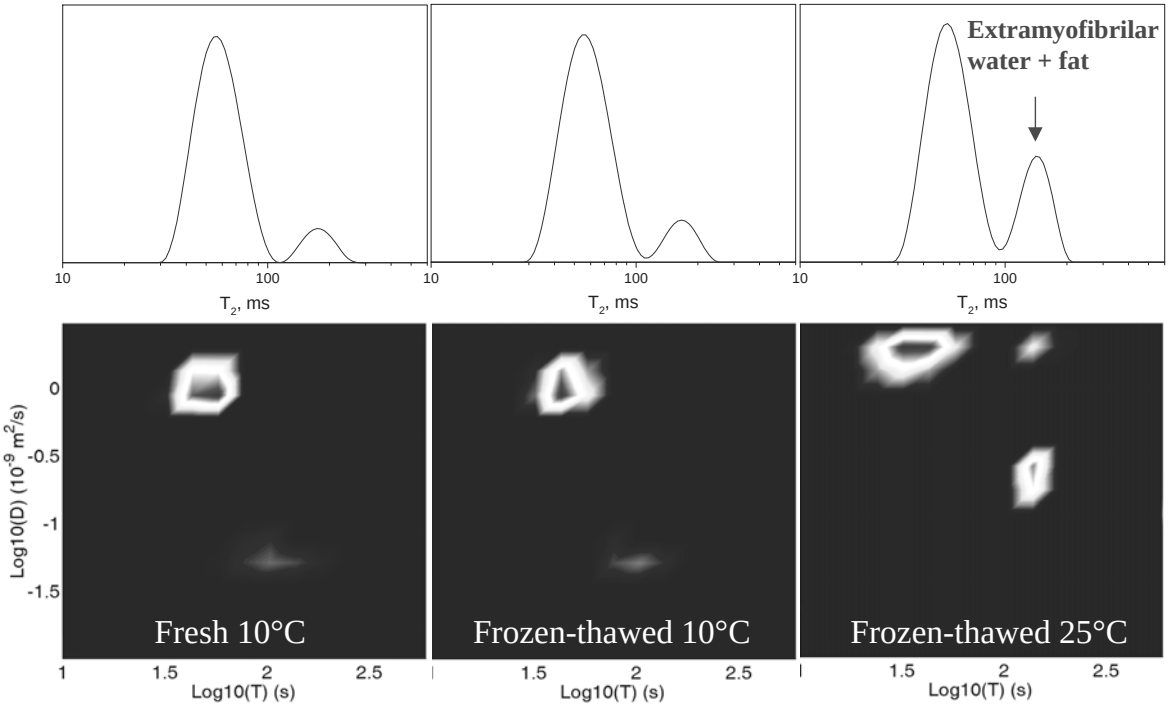

Figure 4 *Diffusion vs. T_2 relaxation time distribution maps (image resolution: 15 × 15 pixels) for fresh (10 ℃) and frozen-thawed (10 and 25 ℃, respectively) Atlantic salmon muscle. Corresponding 1D T_2 distributions are shown at the top of each map.*

3.2 Quantification of fat and water by MRI

Figure 5 shows three types of MRI images acquired in the experiment: 'proton density' image (a), 'fat image' (b) and 'water image' (c). In the 'proton density' image both fat and water components exhibited their maximal intensity. The doped water reference was almost invisible on the 'fat image' - and vice versa - the fat reference was almost invisible on the 'water image' proving a high degree of separation of fat and water. Satisfactory suppression of either the fat or water spectral component could only be achieved in a region with a highly homogeneous magnetic field and RF pulses. Therefore, the MRI instrument had to be carefully shimmed prior to image acquisition. An even better separation between fat and water could be expected when using an NMR instrument with a higher magnetic field due to the increased spectral separation in the frequency domain between fat and water.

The water and fat contents were calculated from the respective MRI images. The average of all slices in case of water and fat were 57 ± 3 % and 19 ± 2 %, respectively. The corresponding values obtained from chemical extraction-based analyses of the same sample were 59 % and 21 %, i.e. within the estimated error of the MRI method. Slightly lower MRI values of both fat and water may be explained by partial suppression of the signal from the observed component and by the roughness of the cut-off algorithm for noise filtering. A possible improvement of the noise filtering method should include extrapolation of the left shoulder of the main peak (see the histogram in Fig.3b) by fitting it with an appropriate model function.

(a) (b) (c)

Figure 5 *Three types of MR images: a) 'proton density' image, b) 'fat image' , and c) 'water image'. Two NMR tubes filled with $MnCl_2$-doped distilled water (upper right) and 100% fish oil (upper left) were used as references*

4 CONCLUSIONS

Compared with conventional 1D relaxation studies, a 2D diffusion weighted relaxation experiment can provide with additional information regarding the presence and mobility of different compounds in biological tissues. At 10^oC, we did not observe significant differences in the 2 D diffusion-relaxation map when fresh and frozen-thawed Atlantic salmon muscle was compared. Subsequent heating to 25 ^oC revealed an additional water component with approximately the same relaxation time as the fat component.

A Chemical Shift Selective MRI protocol (CHESS) was successfully applied to produce separate water and fat images of an Atlantic salmon white muscle. The images were quantified using a simple intensity histogram-based approach. However, more advanced MRI protocols should be evaluated for possible reduction of the magnetic field and RF pulse inhomogeneity effects.

Acknowledgements

Financial support of the Research Council of Norway is gratefully acknowledged. Many thanks to Research Engineer Trond Singstad (St.Olavs Hospital, MR center, Trondheim, Norway) for the technical support and help with optimization of MRI protocols.

References

1 W.C. Cole, A.D. Le Blanc and S.G. Jhingran, *Magn. Reson. Med*., 1993, **29**, 19

2 H.C. Bertram, A.H. Karlsson, M. Rasmussen, O.D. Pedersen, S. Dønstrup and H.J. Andersen, *J. Agric. Food Chem.,* 2001, **49**, 3092

3 E. Veliyulin, C. van der Zwaag, W. Burk and U. Erikson, *"In-vivo determination of fat content in Atlantic salmon (Salmo salar) with a mobile NMR spectrometer"*, Accepted to *J. Sci. Food Agric.*, 2004

4 W. Laurent, J. M. Bonny and J.P. Renou, Quantification of fat and water fractions in high field MRI using a multislice chemical shift selective inversion recovery (CSS-IR). *Proceedings of XVIII-th International conference on Magnetic Resonance in Biological Systems*, Tokyo, Japan, 1998, IV (9), 88.

5 R.V.Mulkern and R.G.S. Spencer , *Magn. Reson. Imaging* , 1988, **6**, 623

6 J.M. Bonny, W. Laurent, R. Labas, R.G. Taylor, P. Berge and J.P. Renou, *J. Sci. Food Agric.*, 2001, **81**, 337

7 L. Tsoref, H. Shinar, Y. Seo, U. Eliav and G. Navon, *Magn. Reson. Med.*, 1998, **30**, 720

8 N. Howell, Y. Shavila, M. Grootveld and S. Williams, *J. Sci. Food Agric*., 1996, **72**, 49

9 M. Hürlimann and L. Venkataramanan, *J. Magn. Reson.*, 2002, **157**, 31

10 S. Godefroy, B. Ryland and P.T. Callaghan, *2D Laplace Inversion*, Victoria University of Wellington, New Zealand, 2003

11 E.G. Bligh and W.J. Dyer, *Can. J. Biochem. Physiol.*, 1959, **37**, 911

12 U. Erikson, E. Veliyulin , T. Singstad and M. Aursand, *J. Food. Sci*., 2004, **69**, 107

13 C. Steen and P. Lambelet, *J. Sci. Food Agric*., 1997, **75**, 268

14 H.C. Bertram, H.J. Andersen and A.H. Karlsson, *Meat. Sci.*, 2001, **57**, 125

Paper III

Water properties and salt uptake in Atlantic salmon fillets as affected by antemortem stress, rigor mortis, and brine salting. A low-field ^{1}H NMR and $^{1}H/^{23}Na$ MRI study

Ida G. Aursand[a, b], Ulf Erikson[a] and Emil Veliyulin[a]

[a] *SINTEF Fisheries and Aquaculture, Brattørkaia 17B, N-7465 Trondheim, Norway*

[b] *Department of Biotechnology, Norwegian University of Science and Technology, Sem Sælandsv. 6/8, N-7491, Trondheim, Norway*

Running title header: NMR studies of salmon muscle

*corresponding author:

Ida Grong Aursand, SINTEF Fisheries and Aquaculture, Brattørkaia 17B, 7465 Trondheim, Norway

Tel: +4798222466, Fax: +47 93 27 07 01, E-mail: Ida.G.Aursand@sintef.no

Abstract

A low-field (LF) ^{1}H NMR T_2 relaxation and ^{23}Na/^{1}H MRI study was performed on Atlantic salmon to study the effect of ante-mortem handling stress and rigor mortis on muscle water properties and subsequent postrigor salting. Compared to rested fish, exhausted fish exhibited a more rapid and stronger development of rigor mortis. This resulted in significant differences in postrigor water holding capacity and salt uptake. By LF NMR T_2 relaxation analysis significant differences in water distribution according to (1) antemortem handling, (2) fillet location, and (3) brine salting were detected. Furthermore, ^{23}Na MRI revealed differences between the two treatments in fillet salt distribution, where the salt penetration in exhausted fillets was more pronounced. By combining ^{1}H and ^{23}Na MR images, the salt diffusion and distribution seemed to be highly affected by the distribution of fat.

Key words: low field NMR, T_2 relaxation, ^{1}H MRI, ^{23}Na MRI, Atlantic salmon, handling stress, water mobility, brine salting, salt distribution

1. Introduction

Present routines for the harvesting of Atlantic salmon (*Salmo salar*) commonly induce handling stress (excessive muscle activity) which in turn will shorten the time to onset of rigor mortis (Erikson, 2001; 2008). In exhausted salmon, rigor onset typically occurs after 2 to 4 h post mortem. If antemortem stress is avoided altogether, rigor onset is delayed for another 20 to 25 h (Erikson, 2001). Stressed fish also develop stronger rigor mortis (Nakayama, Da-Jia & Ooi, 1992) which in turn may also affect quality attributes such as fillet texture (Sigholt, Erikson, Rustad, Johansen, Nordtvedt & Seland, 1997). Due to the rigor contractions, the shape prerigor filleted fillets is different from the postrigor filleted ones, and the irreversible shrinkage in length for anaesthetized and exhausted fillets is 10 % and 7 %, respectively (Misimi, Erikson, Digre, Skavhaug & Mathiassen, 2008).

Water is the major constituent of muscle foods, and the interactions between water and macromolecules determine the water holding properties (Offer & Knight, 1988). The muscle water properties are therefore seen as important quality aspects of muscle food, and the distribution of water in the muscle 3D network is believed to be affected by the physical and biochemical changes in the muscle which occur during for example rigor mortis and subsequent processing such as salting.

Addition of small amounts of NaCl are known to induce swelling of meat (Offer & Trinick, 1983; Offer et al., 1988) and fish muscle (Böcker, Kohler, Aursand & Ofstad, 2008), which is accompanied by changes in muscle water properties such as an increased water holding capacity. The salting process is known to be influenced by raw material characteristics,

such as whether the fish are salted in the pre or postrigor state (Böcker et al, 2008; Aursand, Veliyulin, Böcker, Rustad, & Erikson, 2009), fat and water contents (Gallart-Jornet, Barat, Rustad, Erikson, Escriche & Fito, 2007), and frozen storage (Böcker et al, 2008; Aursand et al, 2009).

Magnetic resonance imaging (MRI) is a powerful imaging modality that can produce high-quality cross-section images of biological systems. Thus, the method can be used for studying chemical and physical properties, anatomical structure, and dynamic processes in foods (Hills, 1998). Many types of contrasts can be produced by the MRI technique using specific MR pulse sequences. This allows differentiation of protons in molecules of different mobility or chemical environment. For example, one can obtain MR images of 'water' and 'fat' (Tingle, Pope, Baumgartner & Sarafis, 1995), or high-resolution images of connective tissue (Bonny, Laurent & Renou, 2001). For fish, MRI is a promising technique that can give a better understanding of *in situ* changes during different processing steps such as freezing, thawing, salting, drying and rehydration. MRI gives a high spatial resolution that allows characterisation of tissue morphology by ^{1}H-MRI. MRI can therefore be useful for the determination of food composition. ^{23}Na MR imaging have been used to follow brine diffusion in cured meat (Renou, Benderbous, Bielicki, Foucat, Donnat, 1994) and in salted cod (Erikson, Veliyulin, Singstad & Aursand, 2004). Earlier ^{23}Na MRI studies on salted lean cod and fatty salmon fillets (skin on) revealed that salt diffusion took place only from the flesh side of the salmon fillets, whereas the cod fillets were salted from both sides suggesting that subcutaneous fat in salmon served as a diffusion barrier (Gallart-Jornet et al, 2007). By the same token, Foucat, Ofstad and Renou (2006) showed by using

^{23}Na MRI that varying fat content along the salmon fillet influenced salt uptake where the anterior part of the fillet gained more salt than the leaner, posterior part.

In recent years, the non-invasive low-field (LF) ^{1}H NMR transversal relaxation (T_2) technique has been used to study water properties in fresh (Jepsen, Pedersen & Engelsen, 1999; Andersen & Rinnan, 2002) frozen/thawed, chilled and processed fish muscle and mince (Jensen, Guldager & Jørgensen, 2002; Løje, Green Petersen, Nielsen, Jørgensen & Jensen, 2007). Nevertheless, few LF NMR studies have been performed on salting of fish (Erikson et al., 2004; Aursand, Gallart-Jornet, Erikson, Axelson & Rustad, 2008; Aursand et al, 2009), and as far as we know, no previous LF NMR studies have investigated fillet water properties as effected by antemortem handling and rigor mortis.

The aim of the present study was to apply non-destructive NMR techniques to improve the understanding as to how ante-mortem handling stress might affect postrigor muscle water properties and salt uptake.

2. Materials and methods

2.1 Fish

Farmed Atlantic salmon (mean weight 4.7 kg, n = 44) fasted for 22 d were netted from the seacage and transported live to our laboratories. At arrival, the fish were transferred in seawater filled 1000-L tubs to 2 holding tanks (4000 L) where the fish, equally distributed among the tanks, were kept for 6 d without feeding. Before slaughter (Day 0), the fish in one of the tanks were anaesthetized. The water supply was stopped and oxygen gas was added. A predefined amount of AQUI-S^{TM} (AQUI-S Ltd., Lower Hutt, New Zealand) was added to give a final concentration of 17 μg L^{-1}. After 16 min, all fish were judged as being fully anaesthetized since they were lying motionless at the bottom of the tank and they did not exhibit regular opercular movements. No vigorous muscle activity took place during the treatment. In the other tank, the fish were chased to exhaustion (30 min). For more details concerning of sampling of fish from the fish farm, transport and keeping the fish at our facilities refer to Erikson, Misimi & Fismen (in press).

Three fish from each treatment were randomly selected and killed by using an *iki jime* tool (AQUI-S, New Zealand), gutted, cleaned (the fish were not bled) and tagged. The white muscle pH, muscle twitches, body temperature, body weight, and fork length were measured. The pooled round weight, length, body temperature, and fillet weight were 4.95 ± 0.13 kg, 77 ± 2 cm, 9.8 ± 0.4 ˚C and 1.50 ± 0.09 kg (mean ± SD, n = 6), respectively. After the assessments, the fish were put on ice in styrofoam boxes for evaluation of rigor mortis. The fish were filleted post-rigor (Day 3) and briefly washed under running tap

water before they were weighed. Samples for different analyses were taken from the anterior (A), mid (B) and posterior (C) parts of the left fillets as shown in Figure 1.

2.2 Muscle twitches

Early postmortem muscle contractions were determined using a Twitch Tester Quality Assessment Tool (AQUI-S Ltd, New Zealand). The instrument measures the electrical excitability of muscle tissues. An electrical pulse was generated (9V DC) by the instrument every 0.6 s. One or a few (< 4) measurements were performed on 1 side of each fish. For each measurement, the electrodes were in contact with the fish for about 1 s. The following scale was devised:

3 - Strong tail twitch (electrodes placed along the entire sideline behind the head and near the caudal fin)

2 - Weak tail twitch (electrodes placed as above)

1 - Minor muscle contractions in (small) restricted areas of the fish surface (electrodes placed a few cm apart)

0 - No contractions whatsoever

2.3 Muscle pH

The pH was measured directly in white epaxial muscle between the sideline and the dorsal fin immediately after killing and after 72 h post-mortem (just before salting). A shielded glass electrode (WTW SenTix 41) connected to a portable pH meter (model WTW 315i; WTW, Weilheim, Germany).

2.4 Body temperature

The fish body temperature was measured immediately after killing in the epaxial muscle using a Testo 110 thermometer (Testo AG, Lenzkirch, Germany).

2.5 Rigor mortis

The development of rigor mortis of gutted fish on ice was carried out using the Rigor Status method with a scale as follows: 0 = pre- or postrigor; 1 = rigor onset (first sign of stiffness, for instance in neck or tail region); 2 = rigor (a larger area is clearly in rigor); 3 = whole fish in rigor; 4 = stronger rigor; [5 = very strong rigor (the fish is extremely stiff, rod-like)] (Erikson, 2001). We wanted to reproduce the extremes of rigor developments, typical of anaesthetized and exhausted fish (Erikson 2001; Misimi et al, 2008). These stress levels are known to produce large differences in myofibrillar tensions during rigor (Nakayama et al. 1992). Our goal was to study whether muscle structure (shrinkage during rigor) would affect salt uptake in salmon fillets (first step in the production of smoked salmon).

2.6 Salting

After postrigor filleting, right fillets (skin on) were immediately immersed in a brine solution of 7.4 % NaCl (w/w) (80 g L^{-1}) at a ratio 1:10 (fish:brine) in closed plastic tanks and kept there for 72 h at 4 ± 1 °C. The brine consisted of ordinary commercial refined salt (Jozo salt, Akzo Nobel Salt, Göteborg, Sweden) and distilled water.

2.7 Water content

The water content before (72 h post mortem) and after salting was calculated after drying duplicates of approximately 2 g of muscle at 105˚C for 24 h. The weight difference of the homogenates before and after drying was considered equal to the total water content of the sample. Samples were taken as shown in Figure 1.

2.8 Water holding capacity

The water holding capacity (WHC) and centrifugation loss were determined on minced muscle by low-speed centrifugation as described by Eide, Børresen and Strøm (1982) with a centrifugation force of 210 g. The WHC is expressed as the percentage of water retained in the mince after centrifugation for 5 min. The analyses were run in quadruplicate, and the calculated mean is reported here. The centrifugation loss was calculated from the same analyses, and is expressed as the difference in weight before and after centrifugation, i.e. total weight loss. Samples were taken as shown in Figure 1.

2.9 Salt content

The NaCl content of the salted fillets was determined using the Volhard method (AOAC, 1990), 2-5 g was weighed accurately into a conical flask, and distilled water (200 mL) was added before the flask was placed in an electric shaker for 45 min. The supernatant (20 mL) was pipetted into Erlenmeyer flasks, and the chloride ions precipitated by adding $AgNO_3$ (0.1 M; 5 to 10 mL). The $AgNO_3$ excess was backtitrated with a NH_4SCN (0.1 M) solution.

A ferric indicator ($FeNH_4(SO_4)_2$) × 12 H_2O in diluted HNO_3) was added for the determination of the endpoint. Samples were taken as shown in Figure 1.

2.10 ^{1}H and ^{23}Na magnetic resonance imaging

After salting, ^{1}H and ^{23}Na MRI measurements were done after salting of anaesthetized and exhausted fillet pieces (Figure 1). Within 3 h after salting the fillet pieces were scanned together with three reference solutions containing 2, 4 and 6 % NaCl w/w. The MRI analyses were carried out at 15°C using a Bruker Avance AV300 multinuclear spectrometer (Bruker Biospin GmbH, Rheinstetten, Germany) with a magnetic field strength of 7 Tesla (300 MHz resonance frequency for ^{1}H). The imaging was performed using a 72 mm double tuned probe $^{1}H/^{23}Na$ and a multi-slice-multi-echo (MSME) imaging protocol. The ^{1}H imaging parameters were the following; echo time = 10 ms, field of view = 6.4 cm, 1 echo, 9 slices, slice thickness = 2 mm, slice separation = 3 mm, number of acquisitions = 1, relaxation delay = 500 ms and a 128 x 128 matrix. The ^{23}Na imaging parameters were the following**:** echo time = 5.6 ms, field of view = 6.4 cm, 1 slice, 5 echoes, slice thickness = 10 mm, number of acquisitions = 128, relaxation delay = 240 ms and a 64 x 64 matrix. In order to see the effect of the chosen slice thickness on the sodium distribution in the ^{23}Na MR image, one of the samples was additionally imaged with a thinner slice of 2 mm. Thinner slice produced much lower signal to noise level which was compensated by increasing the number of acquisitions to 2000 to obtain ^{23}Na image of good quality.

2.11 Low-field ^{1}H NMR

LF ^{1}H NMR measurements were carried out on fillets pieces before (72 h post mortem, Day 3) and after salting (144 h post mortem, Day 6). Three cubes were excised from all fillets (Figure 1). Three subsamples (about 1 × 1 × 3 cm, approximately 2-3 g) were then cut out from each cube, and placed in NMR tubes (diameter 10 mm). The tubes were immediately placed in ice for about 30 min before they were equilibrated to 1˚C in a thermostated water bath (Julabo Labortechnik GmbH, Seelbach, Germany) before analysis. The measurements were performed on a minispec mq 20 (Bruker Optik GmbH, Rheinstetten, Germany) with a magnetic field strength of 0.47 T corresponding to a proton resonance frequency of 20 MHz. The instrument was equipped with a 10 mm temperature-variable probe. A built-in heating element was connected to the temperature control unit (BVT3000, Bruker Optik GmbH). The temperature in the probe was regulated to 4˚C by blowing compressed air through the sample holder. Transversal (T_2) relaxation was measured using the Carr-Purcell-Meiboom-Gill pulse sequence (CPMG) (Carr & Purcell, 1954; Meiboom & Gill; 1958). The T_2 measurements were performed with a time delay between the 90˚ and 180˚ pulses (τ) of 150 μs. Data from 6000 echoes were acquired from 16 scan repetitions. The repetition time between two succeeding scans was set to 4 s. All even echoes were sampled.

2.12 Low-field NMR data processing

The NMR transverse relaxation data were analyzed using two different calculation methods. (1) Multivariate data analysis was performed for all raw relaxation (CPMG) curves. These curves were normalized by setting the first sampled echo to a value of 100, and thereafter scaling the rest of the echo-train. The first 1000 data points were used for the

principal component analysis (PCA) (Jolliffe, 1997) using an in-house made program written in Visual Basic. Each row (n) represented a single fish sample and each column (m) represented a signal amplitude from an echo in the CMPG echo train. Four principal components (k) were used. The input matrix was not mean-centered. (2) Biexponential analysis of T_2 relaxation data was performed by fitting of the following equation to the experimental CPMG curves, similar to that reported by Erikson et al. (2004):

$$Signal = A_{21}e^{-t/T_{21}} + A_{22}e^{-t/T_{22}} \quad \text{(Eq. 1)}$$

where T_{21} and T_{22} were the relaxation components, and A_{21} and A_{22} were the corresponding amplitudes. The calculations were made using MatLab (The Mathworks Inc., Natric, MA). Since the absolute relaxation amplitudes are proportional to the amount of sample (or water and fat) present, the relative amplitudes within samples were used. T_{21} populations were calculated as: $A_{21}/(A_{21} + A_{22})$. For the biexponential fitting, the T_{21} and T_{22} populations sum up to 100%, therefore, only T_{21} population values are given. Three parallel samples from each fish were averaged at both sampling time points. The residuals for the exponential fittings with one, two and three exponents were calculated for varying numbers of sampling points (echoes) (500, 750, 1000, 1250, 1500, 1750, 2000, 2250, 2500, 2750, 3000 and 4000 data points).

2.13 Statistical analysis

Means and standard deviations (SD) are generally shown. The differences in relaxation time between the two raw materials were analyzed by use of ANOVA at a significance level of 95%.

3. Results and discussion

3.1 Defining stress, development of rigor mortis and ultimate pH

The indicators of antemortem stess (muscle twitches and pH) are shown in Table 1. They exhibited the expected differences between treatments in muscle pH (Kieffer, Currie, Tufts, 1994; Erikson, Hultmann & Steen, 2006; Misimi et al, 2008) and muscle twitches (Misimi et al. 2008; Erikson et al, in press) ($P<0.05$). Thus, we had obtained two clearly defined groups that would in turn exhibit two different developments of rigor mortis. Indeed, very different rigor patterns are shown in Figure 2. Rigor onset of the rested fish started after about 25-30 h post mortem and rigor peaked at around 45-50 h, before the fish were in the postrigor state after 55-60 h. In contrast, strenuous antemortem muscle activity lead to rigor onset after about 2 h. Probably, rigor peaked somewhere between 5-10 h, and course of rigor was completed after about 40 h. Notably, anaesthetized fish never attained the strong rigor mortis exhibited by exhausted fish. The different rigor patterns were similar to what we have observed before where salmon were subjected to the same treatments (Erikson 2001; Misimi et al, 2008). Since fish muscle tensions after such treatments are known to be very different during rigor (Nakayama et al., 1992), we hypothesized that flesh microstructure might be altered which in turn would affect fillet salt uptake.

After 3 days post mortem, just before salting, the pH in anaesthetized fillets was still slightly higher than in exhausted fillets ($P<0.05$; Table 1).

3.2 Water content, water holding capacity and salt content

The water contents at fillet locations A, B and C, before (Day 3) and after (Day 6) salting are shown in Table 1. Antemortem stress did not seem to have any affect water contents, except for in the anterior part (location C), where the water content of exhausted fish was significantly higher ($P<0.05$). However, due to the uneven fat distribution in salmonids (Katikou, Hughes & Robb 2001), such comparisons must be done with caution unless both fat and water contents in the same sample is known. Since we did not analyse the fat content in our samples, it is likely that our water data basically reflected the fat distribution pattern rather the potential effects of stress. For both treatments however, there seems to be a trend towards higher water contents after salting. In this comparison, the samples were taken from exactly the same area of right and left fillets from the same fish, one unsalted, the other one after addition of salt. Using the fat-water correlations given by Katikou et al. (2001), the total fat contents of our unsalted fillets were around 9, 6 and 2 % for location A, B and C, respectively.

At location A, before salting, the anaesthetized fillets had a significantly higher WHC (96.5 %) than their exhausted counterparts (94.9 %, Table 1). After salting, the WHC of anaesthetized and exhausted fillets increased by 1.0 and 2.5 % points, respectively, and the difference was no longer significant. The exhausted fillets gained significantly more salt (1.6 % NaCl) at location A than the anaesthetized fillets (1.2 % NaCl, Table 1).

Taken together, both the WHC data and the salt contents support our hypothesis that the stronger rigor contractions in stressed fish affected the muscle cell structure or the protein

network in such a way that the mobile water was easier lost when a physical force was applied during centrifugation. This might also have altered the salt diffusion rate into the fillets.

3.3 MRI – macroscopic structure and salt distribution

Figure 3 shows the ^{1}H and ^{23}Na MR images of the same slice of anaesthetized and exhausted fillet pieces excised from the anterior region (location C) of the fillets. In the ^{1}H MR images (b, d and f), the subcutaneous fat layer is evident (top of fillet piece) along with the myocommata, containing both collagen (invisible in our MR images) and fat (light stripes). These features were most clearly visible in Figure 3 (a) where a ^{23}Na MR image of a thinner slice (2 mm) was acquired with considerably longer acquisition time to improve sodium resolution. When comparing the ^{23}Na and the ^{1}H MR images (image a and b, respectively) it is evident that the myocommata area with a high fat content (shown as 'light stripes'), were not significantly invaded by sodium, since in the ^{23}Na MR image, the area of myocommatas are visible as 'black stripes', indicating low salt areas. Furthermore, the ^{23}Na MR images (Figure 3 (a) (c) and (e)) show that the highest salt content was observed near the surface of the fillet with a gradual decrease inwards. This was partly because of the presence of the skin, acting as a diffusion barrier (Gallart-Jornet et al, 2007). It was evident that the salt had penetrated deeper into the exhausted fillets than into the anaesthetized fillets. These results are well supported by a higher salt content in exhausted fillets found by chemical analysis (Table 1). The fact that the ^{23}Na MR images revealed a deeper salt penetration into the exhausted fillets compared to the anaesthetized ones support our hypothesis that stronger rigor contractions in exhausted fish had an effect on the muscle

microstructure. This assumption is also supported by an earlier study (Aursand et al, 2009), where prerigor, postrigor and frozen-thawed salmon flesh was compared. It was shown by light microscopic analyses that a more open muscle microstructure found lead to a more rapid salt uptake.

Sodium concentration profiles of the salmon fillets along with a reference solution containing 4% NaCl are presented in Figure 4. The calculation of sodium profiles was based on averaging of ^{23}Na intensities in the MR images in a direction perpendicular to the fillet thickness within a selected rectangular region of interest (ROI) (as shown in Figure 3). The minor displacements along the axis "position" were due to the difference in fillet thicknesses at each sampling time. Considering the absolute values of NaCl, it should be realized that the MRI approach used here (spin-echo) detected mainly free sodium. A fraction of bound sodium is not detected (Veliyulin & Aursand, 2007). However, our samples contained relatively low amounts of salt, and sodium invisibility is known to increase with increasing salt content (Veliyulin & Aursand, 2009). Moreover, in the present study, a comparison of sodium distribution was the main aim, and it is our belief that sodium invisibility does not affect our conclusions. Small differences in the average salt uptake between the three fillet pieces were observed, but still significant differences in the salt uptake of the two treatments was observed.

3.4 Low-Field ^{1}H NMR – water dynamics

To examine water mobility and water distribution in the fillets, the LF ^{1}H NMR T_2 relaxation times were measured. The data was processed in two different ways.

3.4.1 Principal Component Analysis

The overall variation in the NMR relaxation data of the anaesthetized and exhausted fillets were analyzed by performing a principal component analysis (PCA) on samples taken before and after salting separately (Figure 5). The relaxation curves were normalized against the maximum amplitude. In this way, potential differences in total water content did not contribute to the weighting of samples in the PCA score plot. In the comparison of unsalted anaesthetized and exhausted fillets, an evident separation between T_2 relaxation data of the two treatments was seen. Subsequently, the effect of salt uptake (1-2 %) was much stronger than the effect of antemortem stress, as the separation due to different treatments in the T_2 relaxation data were not seen after brine salting. In both cases, dispersion within each group was observed. This might be explained by varying fat content along the fillet. Location on the fillet had an effect on T_2 relaxation both before and after salting, the posterior part (location C) separated from the anterior and mid part of the fillets (location A and B, respectively).

3.4.2 Exponential fitting

In Table 2, relaxation times and corresponding populations found by biexponential fitting are shown. When examining these data, one should remember that this form of data processing forces the curve to fit to two exponents. However, the method is simple and robust, and it has traditionally been used to interpret T_2 relaxation data. Mono- and triexponential fitting of the data set was also approached. The residuals of fittings to one, two and three exponents are presented in Figure 6. As can be seen, one exponent gave the

poorest fit. Increasing to two exponents gave an evident improvement, whereas no visible improvement of the fit quality was seen after including of the third exponential component, indicating that a biexponential model was sufficient to adequately describe the relaxation curves.

The fastest relaxing component (T_{21}) revealed mean relaxation times in the range of 46-56 ms before salting and 51-74 ms after salting, whereas the slower relaxing component (T_{22}) had mean relaxation times between 155-216 and 134-152 ms before and after salting, respectively. These values are in agreement with our earlier T_2 relaxation studies of Atlantic salmon postrigor muscle (Aursand et al, 2008, Aursand et al, 2009). Jepsen et al (1999) reported a similar value for the T_{21} relaxation component (49 ms) and a longer T_{22} relaxation time (252 ms) in postrigor salmon muscle. Løje et al (2007) reported three T_2 components with values of 39, 85 and 353 ms in raw salmon by using PARAFAC modelling. The differences in the reported values might be due to differences in fillet composition (fat) and structure as affected by factors such as feed composition, feeding regimes, ante- or postmortem handling and storage time or the method of T_2 data analysis.

3.4.3 T_2 relaxation and microstructure

The majority (92 – 98 % in unsalted fillets; Table 2) of the population of water molecules revealed relaxation behaviour characterized by the T_{21} relaxation time constant. An earlier study on pork, Bertram, Purslow and Andersen (2002) reported correlation ($r = 0.84$) between the T_{21} time constant and the muscle tissue sarcomere length. They suggested that the structural features associated with changes in sarcomere length directly affected the

water mobility characterized by the T_{21} time constant. Based on these results, they suggested that the T_{21} component reflected water located within highly organized myofibrillar protein structures. Compared with our unsalted salmon fillets, the anaesthetized ones had a significantly larger T_{21} population, and a corresponding lower T_{22} population than the exhausted fillets. If we suppose that the assumptions based on pork tissue are applicable to salmon muscle, our T_{21} values indicate that in the anaesthetized tissues, more water was kept within such organized protein structures than in the exhausted tissue. These results are in agreement with our hypothesis that excessive antemortem stress with subsequently stronger rigor contractions (Figure 2) resulted in pronounced changes in tissue structure. In turn, this affected water distribution within the tissue network in such a way that the overall water mobility was increased.

In an earlier study on cod fillets, Andersen & Rinnan (2002) reported a larger T_{21} population in the anterior region of the fillet, whereas samples from the tail part had a larger T_{22} population. It was suggested that this might be due to decrease in cell and fibre size backwards the fillet. These differences in T_2 populations were not seen in our data. However, it must be taken into account that in salmon tissues, the T_{22} relaxation time constant reflects both fat and water protons (Veliyulin, Aursand & Erikson, 2005), whereas in lean cod tissue, only water protons give rise to the NMR signal. For both treatments, we observed a significantly higher T_{21} relaxation time in the tail region (location C) compared to the anterior and mid region (locations A and B). This indicates increased water mobility, possibly due to the higher water content in the tail region.

After salting, a shift towards longer T_{21} relaxation times coupled with a decrease in the T_{21} population was observed both for both treatments. The observations are in agreement with earlier studies of cod and salmon (Aursand et al, 2008), and pork (Wu et al, 2006) demonstrating a coupling between increased T_{21} relaxation times and salt-induced swelling of the myofibers.

After salting, no significant differences in the T_{21} relaxation time constants due to antemortem handling were observed. Consequently the anticipated differences in muscle structure were smoothed out by the uptake of salt. However, sampling location was still an issue for both treatments. After salting, the longest T_{21} relaxation component was still observed in the posterior part of the fillet (location C). This effect was even more pronounced than in unsalted fillets. In a previous studies (Foucat et al, 2006; Aursand et al, 2009), a higher salt uptake in the posterior part has been reported. Both in pork (Wu et al, 2006), and cod and salmon (Aursand et al, 2008; 2009), an increase in the relaxation time constant as a function of addition of small amounts of NaCl has been found. The changes in the T_{21} relaxation time constant were coupled with salt-induced swelling of the myofibers. Consezuently, we may assume that, a higher NaCl uptake in the posterior part of the fillet resulted in a higher degree of swelling, which in turn resulted in a pronounced shift towards a longer T_{21} relaxation times.

3.5 Conclusions

By LF NMR T_2 relaxation analysis we were able to significantly detect differences in water distribution according to (1) antemortem handling, (2) fillet location, and (3) brine salting.

^{23}Na MRI revealed in salt distribution differences between anaesthetized and exhausted fillets, where the salt penetration in the latter fillets was more pronounced. By combining ^{1}H and ^{23}Na MR images, the salt diffusion and distribution was shown to be highly affected by the distribution of fat.

Acknowledgements

This research was conducted as a part of the Matforsk-SINTEF Strategic Institute Programme "Production improvements of salted/cured meat and fish: Development of rapid and non-destructive salt analyses related to production, yield and quality (Project no. 153381/140)" supported by the Research Council of Norway. The authors would like to thank Dr. Vegar Johansen and Dr. David E. Axelson for their support and valuable participation in discussions regarding LF NMR data analysis.

Literature cited

Andersen, C.M. & Rinnan, Å. (2002) Distribution of water in fresh cod. *Lebensmittel-Wissenshaft und Technologie,* 35, 687-696.

[AOAC] Assn. of Official Analytical Chemists (1990) Official methods of analysis. Vol. 2. 15th ed. Arlington, Va.: AOAC. (pp 810).

Aursand, M., Bleivik, B, Rainuzzo, J.R, Jørgensen, L & Mohr, V. (1994) Lipid distribution and composition of commercially farmed atlantic salmon (Salmo salar). *Journal of the Science of Food and Agriculture,* 64, 239-248.

Aursand I.G. , Veliyulin, E., Böcker U., Rustad, T. and Erikson, U. (2009) Water and salt distribution in Atlantic salmon (*Salmo salar*) studied by low-field ^{1}H NMR, ^{1}H and ^{23}Na MRI and light microscopy – Effects of raw material quality and brine salting. *Journal of Agricultural and Food Chemistry,* **57**, 46-54.

Aursand, I.G., Gallart-Jornet, L., Erikson, U., Axelson D.E. & Rustad, T. (2008) Water distribution in brine salted cod (*Gadus morhua*) and salmon (*Salmo salar*): A low-field ^{1}H NMR study. *Journal of Agricultural and Food Chemistry,* 56, 6252-6260.

Bertram, H.C., Purslow, P.P., & Andersen, H.J. (2002) Relationship between meat structure, water mobility and distribution—a low field NMR study. *Journal of Agricultural and Food Chemistry,* 50, 824–829.

Bonny, J.M., Laurent, W. & Renou, J.P. (2001) Characterisation of meat structure by NMRimaging at high field, in *Magnetic Resonance in Food Science: A View to the Future*, ed. by Webb GA. Royal Society of Chemistry, Cambridge, UK, (pp 17–21).

Böcker, U., Kohler, A., Aursand, I.G. & Ofstad, R. (2008) Effects of brine salting with regard to raw material variation of Atlantic salmon (*Salmo salar*) Muscle

Investigated by Fourier Transform Infrared Microspectroscopy. *Journal of Agricultural and Food Chemistry,* 56, 5129-5137.

Carr, H.Y. & Puncell, E.M. (1954) Effects of diffusion on free precession in nuclear magnetic resonance experiments. *American Journal of Physiology*, 94, 630-638.

Eide, O., Børresen, T. & Strøm, T. (1982) Minced fish production from capelin (*Mallotus* V*illosus*). A new method for gutting, skinning and removal of fat from small fatty fish species. *Journal of Food Science,* 47, 347-349, 354.

Erikson, U. (2008) Live chilling and carbon dioxide sedation at slaughter of farmed Atlantic salmon: A description of a number of commercial case studies. *Journal of Applied Aquaculture,* 20, 38-61.

Erikson, U. (2001) Rigor measurements. In: *Farmed Fish Quality* (S. Kestin and P. Wariss, Eds.), Blackwell Science, Oxford, UK (pp 283-297).

Erikson, U., Hultmann, L. & Steen, J.E. (2006). Live chilling of Atlantic salmon (*Salmo salar*) combined with mild carbon dioxide anaesthesia. I. - Establishing a method for large-scale processing of farmed fish. *Aquaculture* 252: 183-198.

Erikson, U. & Misimi, E. (2008) Atlantic salmon skin and fillet color as affected by perimortem handling stress, rigor mortis and ice storage. *Journal of Food Science*, 73, C50-C59.

Erikson, U., Veliyulin, E., Singstad, T. & Aursand, M. (2004) Salting and desalting of fresh and frozen-thawed cod (*Gadus morhua*) fillets: A comparative study using ^{23}Na NMR, ^{23}Na MRI, low-field ^{1}H NMR, and physicochemical analytical methods. *Journal of Food Science*, 69, 107-114.

Foucat, L., Ofstad, R. & Renou, J.-P. (2006) How is the fish meat affected by technological processes? In: *Modern Magnetic Resonance* (G. A. Webb, Ed.) Springer, The Netherlands, 957-961.

Gallart-Jornet, L., Barat, J.M., Rustad, T., Erikson, U., Escriche, I. & Fito, P. (2007) A comparative study of brine salting of Atlantic cod (*Gadus morhua*) and Atlantic salmon (*Salmo salar)*. *Journal of Food Engineering,* 79, 261-270.

Hills, B. (1998). *Magnetic Resonance Imaging in Food Science*. Wiley, New York (pp. 96).

Jensen, K.N., Guldager, H.S. & Jørgensen B.M. (2002) Three-way modelling of NMR relaxation profiles from thawed cod muscle. *Journal of Aquatic Food Product Technology,* 11, 201-214.

Jepsen, S.M., Pedersen, H.T. & Engelsen, S.B. (1999) Application of chemometrics to low-field ^{1}H NMR relaxation data of intact fish flesh. *Journal of the Science of Food and Agriculture,* 79, 1793-1802.

Jolliffe, I.T. (1997) *Principal Component Analysis*. Springer-Verlag: Berlin, Germany.

Kieffer, J.D., Currie, S., Tufts, B.L. (1994). Effects of environmental temperature on the metabolic and acid-base responses of rainbow trout to exhaustive exercise. *Journal of Experimental Biology*, 194, 299–317.

Løje, H., Green Petersen, D., Nielsen, J., Jørgensen, B.M. & Jensen, K.N. (2007) Water distribution in smoked salmon. *Journal of the Science of Food and Agriculture*, 87, 212-217.

Meiboom, S. & Gill, D. (1958) Modified spin-echo method for measuring nuclear times. *Review of Scientific Instruments*, 29, 688-691.

Katikou, P., Hughes, S.I. & Robb, D.H.F. (2001) Lipid distribution within Atlantic salmon (*Salmo salar*) fillets. *Aquaculture,* 202, 89-99.

Misimi, E., Erikson, U., Digre, H., Skavhaug, A. & Mathiassen, J.R. (2008) Computer vision-based evaluation of pre- and postrigor changes in size and shape of Atlantic cod (*Gadus morhua*) and Atlantic salmon (*Salmo salar*) fillets during rigor mortis and ice storage: Effects of perimortem handling stress. *Journal of Food Science,* 73, E57-E68.

Nakayama, T., Da-Jia, L., & Ooi, A. (1992) Tension changes of stressed and unstressed carp muscle isometric rigor contraction and resolution. *Nippon Suisan Gakkaishi,* 58, 1517–1522.

Offer, G. & Knight, P. (1988) The structural basis of water-holding in meat Part 1: General principles and water uptake in meat processing. In *Developments in Meat Science*; Lawrie, R., Ed.; Elsevier Science Publishers Ldt: Barking, Essex, UK, vol. 4, (pp 63-172).

Offer, G. & Trinick, J. (1983) On the mechanism of water holding in meat: the swelling and shrinking of myofibrils. *Meat Science*, 8, 245-281.

Renou, J.P., Benderbous, S., Bielicki, B., Foucat, L. & Donnat, J.P. (1994) ^{23}Na magnetic resonance imaging: distribution of brine in muscle. *Magnetic Resonance Imaging* 12, 131–137.

Sigholt, T., Erikson, U., Rustad, T., Johansen, S., Nordtvedt, T.S. & Seland, A., (1997) Handling stress and storage temperature affect meat quality of farm-raised Atlantic salmon (Salmo salar). *Journal of Food Science,* 62, 898–905.

Tingle, J.M., Pope, J.M., Baumgartner, P.A. & Sarafis, V (1995) Magnetic resonance imaging of fat and muscle distribution in meat. *International Journal of Food Science and Technology,* 30, 437–446.

Veliyulin, E., Aursand, I.G. & Erikson, U. (2005) Study of fat and water content in Atlantic salmon (*Salmo salar*) by low-field NMR and MRI. In: *Magnetic Resonance in Food Science – The multivariate Challenge* (S.B. Engelsen, P.S. Belton and H.J. Jakobsen Eds.), pp 148-155, Special Publication No. 299, The Royal Society of Chemistry, Cambridge.

Veliyulin, E. & Aursand, I.G. (2007) ^{1}H and ^{23}Na MRI studies of Atlantic salmon (Salmo salar) and Atlantic cod (*Gadus morhua*) fillet pieces salted in different brine concentrations, *Journal of the Science of Food and Agriculture*, 87, 2676–2683.

Wu, Z. Y., Bertram, H. C., Kohler, A., Bocker, U., Ofstad, R. & Andersen, H. J. (2006) Influence of aging and salting on protein secondary structures and water distribution in uncooked and cooked pork. A combined FT-IR microspectroscopy and H-1 NMR relaxometry study. *Journal of Agricultural and Food Chemistry,* 54, 8589–8597.

Figure captions

Figure 1: Sampling locations for the various analyses of the Atlantic salmon fillets: anterior (A), mid (B) and posterior (C) fillet regions. For details, see text.

Figure 2: Development of rigor mortis of anaesthetized and exhausted Atlantic salmon during ice storage.

Figure 3: Sodium (^{23}Na) and proton (^{1}H) magnetic resonance images from the same cross-sectional slice of brine salted anaesthetized and exhausted Atlantic salmon fillet pieces. Reference solutions (2, 4 and 6 % NaCl) are shown as circles (10 mm tubes cross sections) in the lower part of each image. Lighter areas in the ^{1}H MR images correspond to fat rich areas. The image slice thicknesses were 2 mm for image (a) and (b), and 10 mm for the latter ones. The selected region of interest (ROI) indicates the area used for calculation of profiles in Figure 4.

Figure 4: ^{23}Na MRI concentration profiles through brine salted anaesthetized and exhausted Atlantic salmon fillets after brine salting in 7.8 % NaCl for 3 days. The skin side of the fillet pieces were in all cases placed opposite to the reference glass container with a 4 % NaCl solution (to the right in the figure). The selected region of interest (ROI) for calculation of the profiles is shown in Figure 3.

Figure 5: PCA score plots of T_2 relaxation data of anaesthetized and exhausted fillets before and after salting separately. In the upper panel of the figure, samples are labelled by ante-

mortem handling (exhausted unsalted (E0), anaesthetized unsalted (U0), exhausted salted (SS) and anaesthetized salted (US)). In the lower panel, samples are labelled by fillet sampling location (anterior part unsalted (A0), mid part unsalted (B0), posterior part unsalted (C0), anterior part salted (AS), mid part salted (BS) and posterior part salted (CS)).

Figure 6: Normalized residuals of mono-, bi- and three exponential fitting to varying number of echoes (500 – 4000) of T_2 relaxation curves obtained from post-mortem Atlantic salmon muscle (anterior region, A) exposed to ante-mortem stress (n=6). Maximum and minimum residuals for each sample are indicated.

Table captions

Table 1: Definition of two levels of handling stress in Atlantic salmon white muscle twitches and initial pH. Postrigor pH, salt content, water content and water holding capacity of unsalted (0) and salted (S) anaesthetized and exhausted fillets are also shown.

Table 2: Transversal relaxation times, T_{21} and T_{22} and corresponding relative T_{21} populations obtained from unsalted (0) and salted (S) anaesthetized and exhausted Atlantic salmon fillets. Mean (SD, n= 9 - 12).

Figures

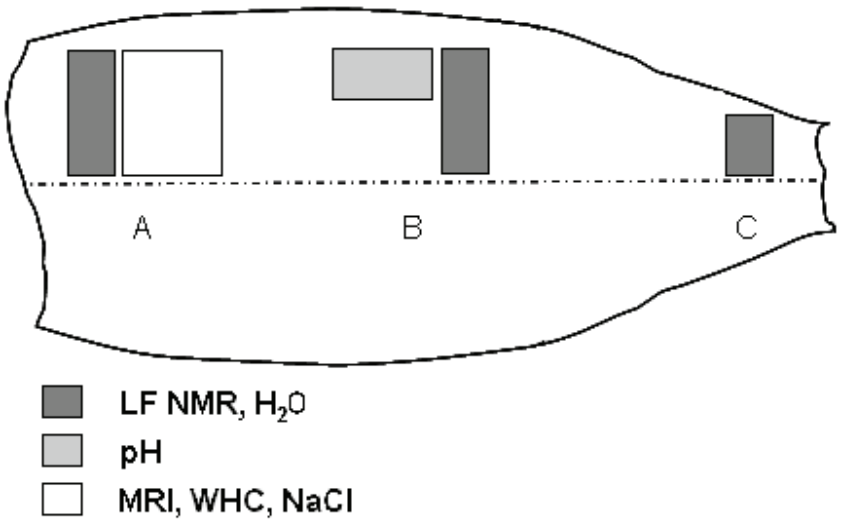

Figure 1

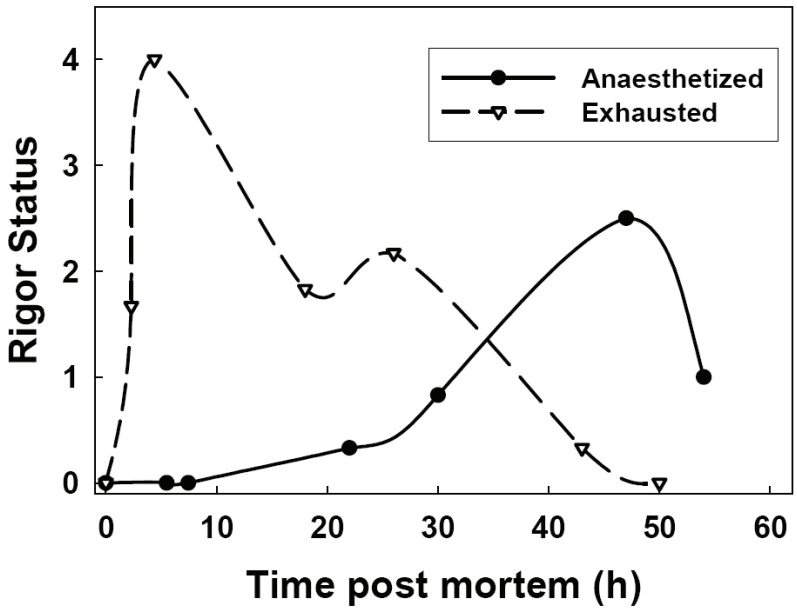

Figure 2

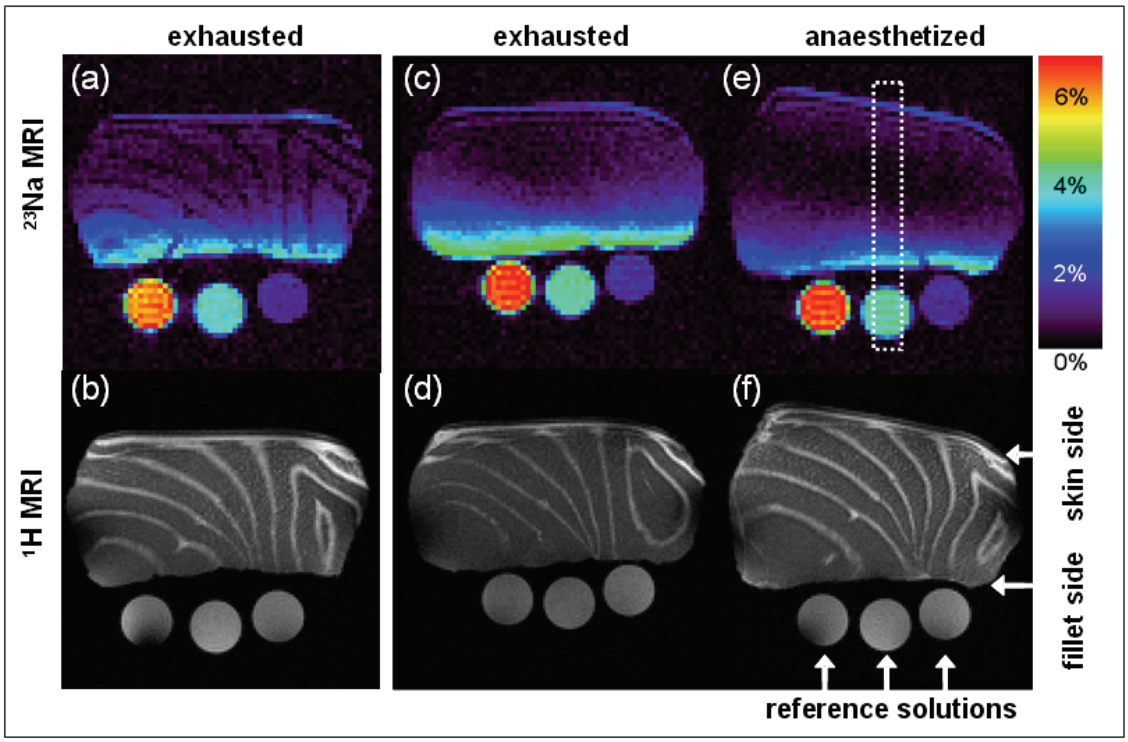

Figure 3

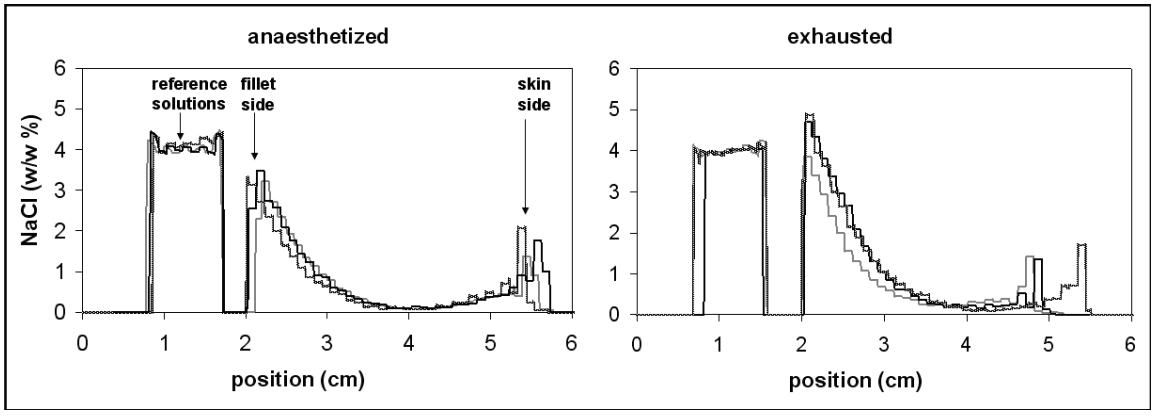

Figure 4

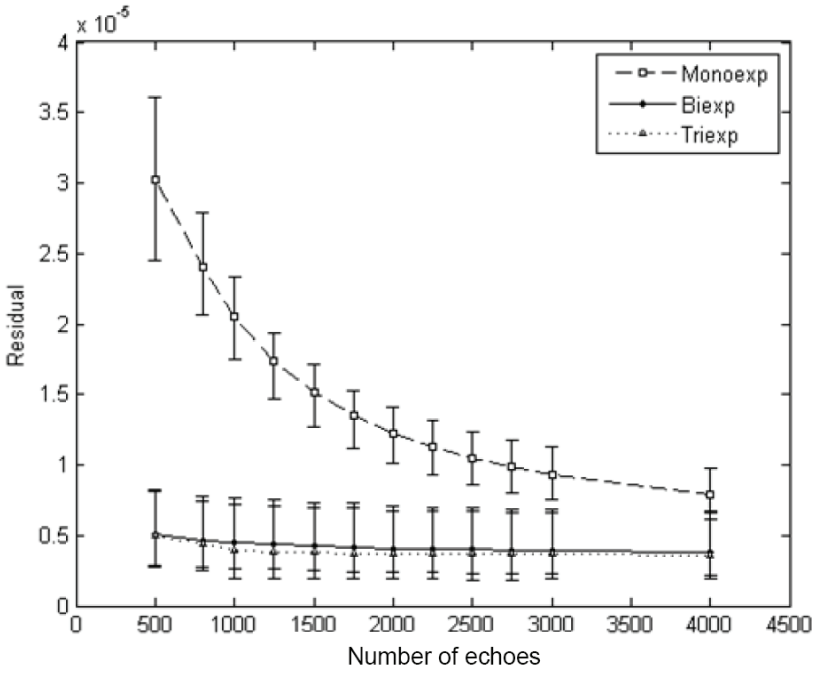
x 10^-5
Residual
Number of echoes
Monoexp
Biexp
Triexp
0
0.5
1
1.5
2
2.5
3
3.5
4
0
500
1000
1500
2000
2500
3000
3500
4000
4500

Figure 5

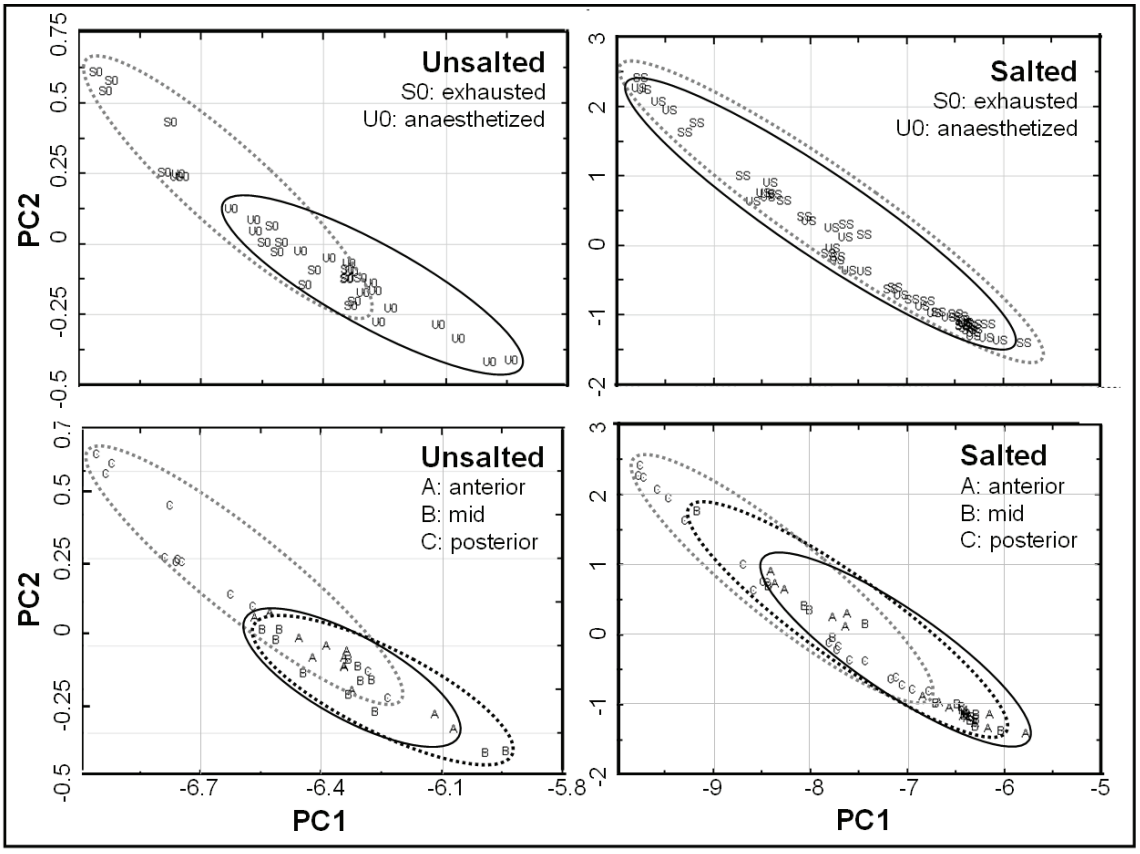
Unsalted
S0: exhausted
U0: anaesthetized
Salted
S0: exhausted
U0: anaesthetized
Unsalted
A: anterior
B: mid
C: posterior
Salted
A: anterior
B: mid
C: posterior
PC2
PC1
PC2
PC1

Figure 6

Tables

Table 1

treatment (fillet location)	twitch tester (range: 0-3)[I]	initial pH[I]	ultimate pH[II]	$H_2O_{(0)}$ (%)	$H_2O_{(S)}$ (%)	$WHC_{(0)}$ (%)	$WHC_{(S)}$ (%)	NaCl (%)
anaesthetized (A)	NA	NA	NA	68.8(1.4)^{CD}	69.0(1.9)^{BC}	96.5(0.7)^{B}	97.5(0.8)*	1.2(0.1)^{A}
anaesthetized (B)	3.0(0.0)^{A}	7.3(0.1)^{A}	6.5(0.0)^{A}	70.3(0.2)^{C}	73.1(0.5)^{B}*	NA	NA	NA
anaesthetized (C)	NA	NA	NA	74.2(0.5)^{B}	78.0(0.9)^{A}*	NA	NA	NA
exhausted (A)	NA	NA	NA	68.0(0.8)^{D}	69.2(0.6)^{C}*	94.9(1.2)^{A}	97.4(1.0)*	1.6(0.3)^{B}
exhausted (B)	0.7(0.9)^{B}	6.7(0.0)^{B}	6.4(0.0)^{B}	70.8(0.9)^{BC}	73.6(0.9)^{B}*	NA	NA	NA
exhausted (C)	NA	NA	NA	76.1(1.0)^{A}	76.9(1.0) ^{A}	NA	NA	NA

(^{I}) analyses were performed less than 1 min post mortem

(^{II}) analyses were performed 3 days post mortem, before salting

Water content subscript 'O' or 'S' refer to before and after salting, respectively. Different letters (A, B, C or D) indicate significant differences between treatments ($P<0.05$). The asterisk (*) indicates significant differences between unsalted and salted fillets ($P<0.05$). NA = Not Analyzed.

Table 2

treatment (fillet location)	$T_{21(0)}$ (ms)	$T_{21(S)}$ (ms)	$T_{22(0)}$ (ms)	$T_{22(S)}$ (ms)	T_{21} $pop_{(0)}$ (%)	T_{21} $pop_{(S)}$ (%)
anaesthetized (A)	$48.1(3.2)^{A}$	$52.9(6.1)^{A}$	169.6(16.1)	$144.7(10.8)^{A}$	$95.7(0.8)^{A}$	83.2(14.7)
anaesthetized (B)	$46.0(2.8)^{A}$	$52.4(7.4)^{A}$	159.6(10.5)	$144.0(12.6)^{A}$	$95.7(0.9)^{A}$	84.3(14.0)
anaesthetized (C)	$52.6(3.5)^{BC}$	$74.4(13.4)^{B*}$	216.1(47.3)	$152.3(32.1)^{B*}$	$97.6(0.7)^{A}$	$69.8(12.3)^{*}$
exhausted (A)	$48.8(0.9)^{AB}$	$50.9(8.0)^{A}$	160.7(23.9)	$134.0(19.9)^{A}$	$95.5(1.6)^{A}$	$78.7(14.6)^{*}$
exhausted (B)	$49.1(1.2)^{AB}$	$51.9(5.2)^{A}$	187.0(26.7)	$137.9(12.9)^{AB*}$	$96.3(1.1)^{A}$	85.9(11.5)
exhausted (C)	$56.2(1.0)^{C}$	$67.6(13.2)^{B*}$	154.9(30.5)	$143.3(34.3)^{A}$	$92.2(3.9)^{B}$	$77.3(12.1)^{*}$

Subscripts 'O' or 'S' refer to before and after salting, respectively. Different letters (A, B, C) indicate significant differences between fillet locations and antemortem stress ($P<0.05$) The asterisk (*) indicates significant differences between unsalted and salted fillets ($P<0.05$)

Paper IV

)ó Î Ïô ÉÎÃÌÕÄÅÄ ÄÕÅ ôÏ ÃÏÐÙÒÉÇÈÔ

Paper V

)ó Î Ïô ÉÎÃÌÕÄÅÄ ÄÕÅ ôÏ Ã ÏÐÙÒÉÇÈÔ